

Massimo Persic
INAF+INFN Trieste



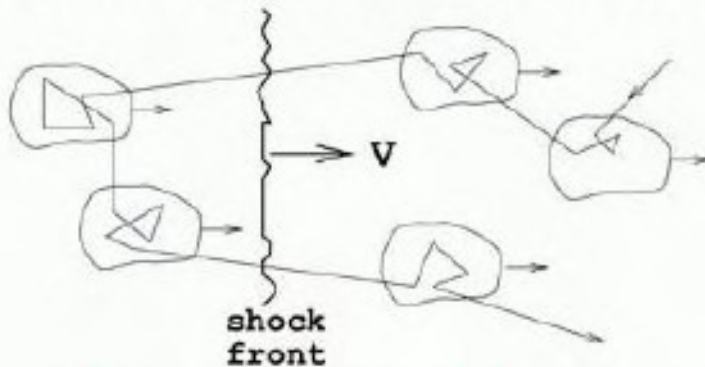
Gamma Rays
from Star Forming Galaxies
and Dark Matter

Non-Thermal plasma: $T_{\text{ion}} \neq T_{\text{electron}}$
 $f(\mathbf{v})$ of either species non-Maxwell Boltzmann

Particle Acceleration

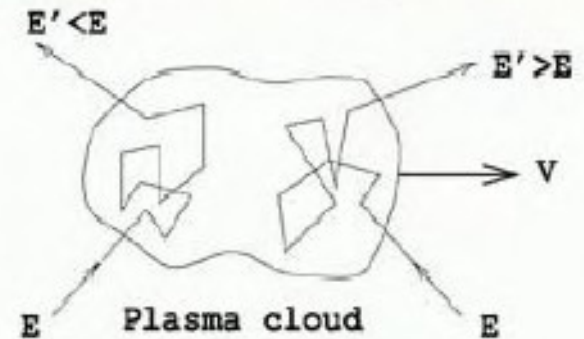
Fermi Acceleration Mechanism Stochastic energy gain in collisions with plasma clouds

1st order :
 acceleration in strong shock wave
 (supernova ejecta, RG hot spots...)



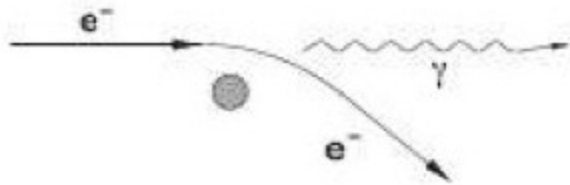
$$\frac{\Delta E}{E} \sim \beta \quad \beta = \frac{v}{c} \lesssim 10^{-1}$$

2nd order :
 randomly distributed magnetic mirrors

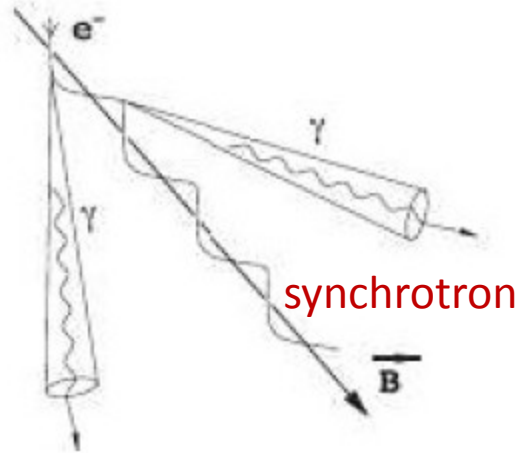


$$\frac{\Delta E}{E} \sim \beta^2 \quad \beta = \frac{v}{c} \lesssim 10^{-4}$$

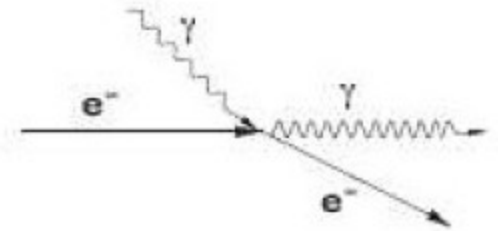
Radiation Processes



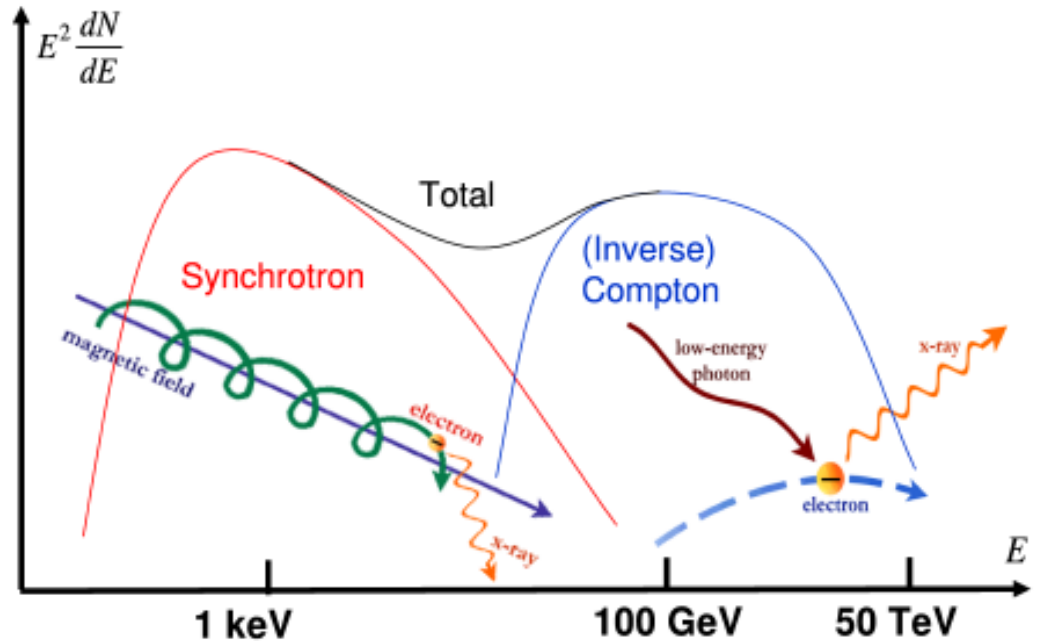
bremsstrahlung

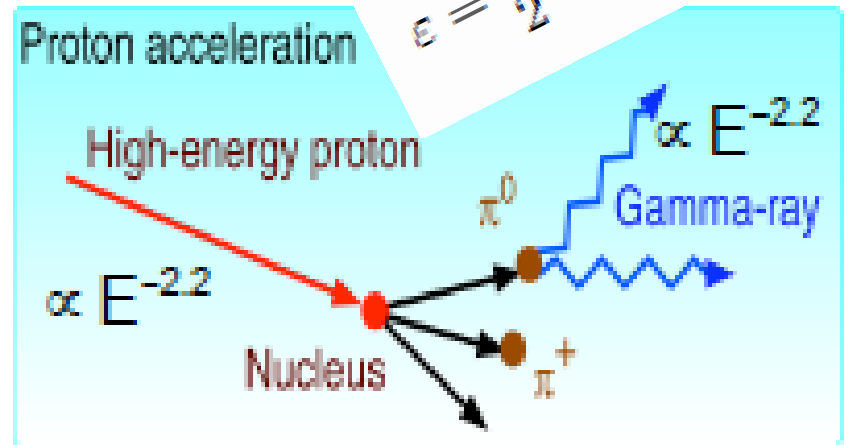
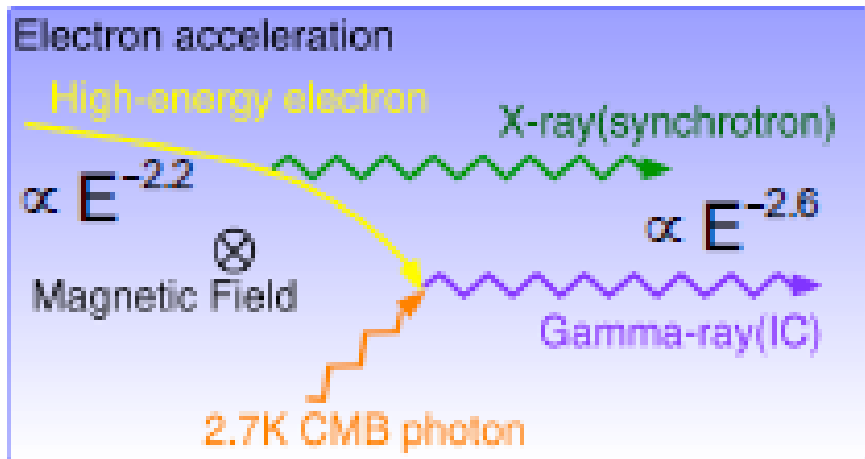


synchrotron

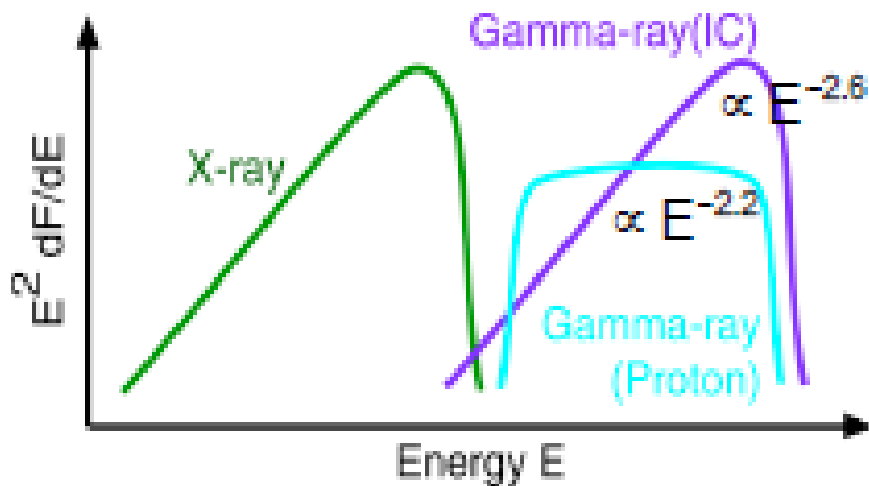


Inverse Compton



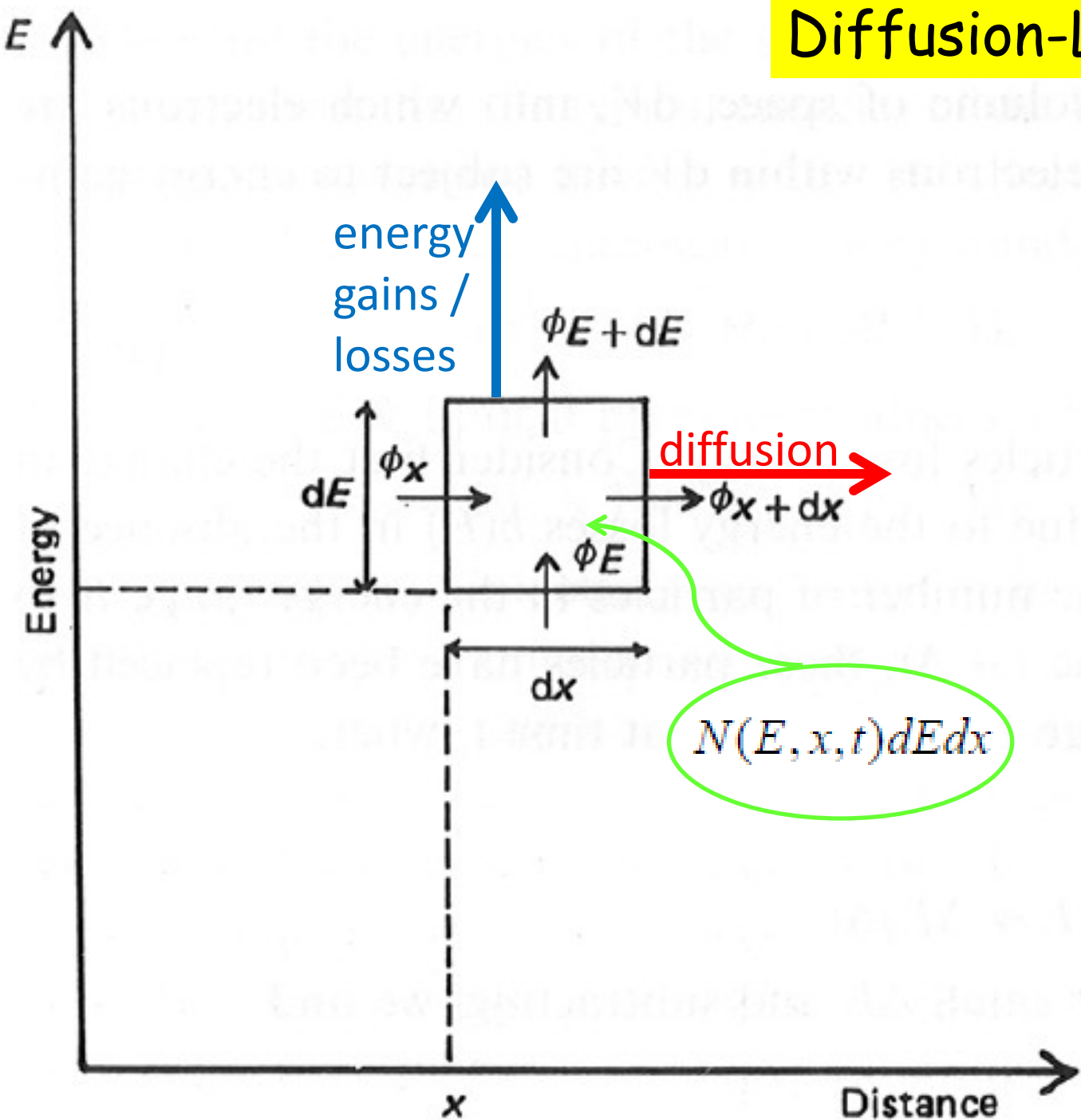


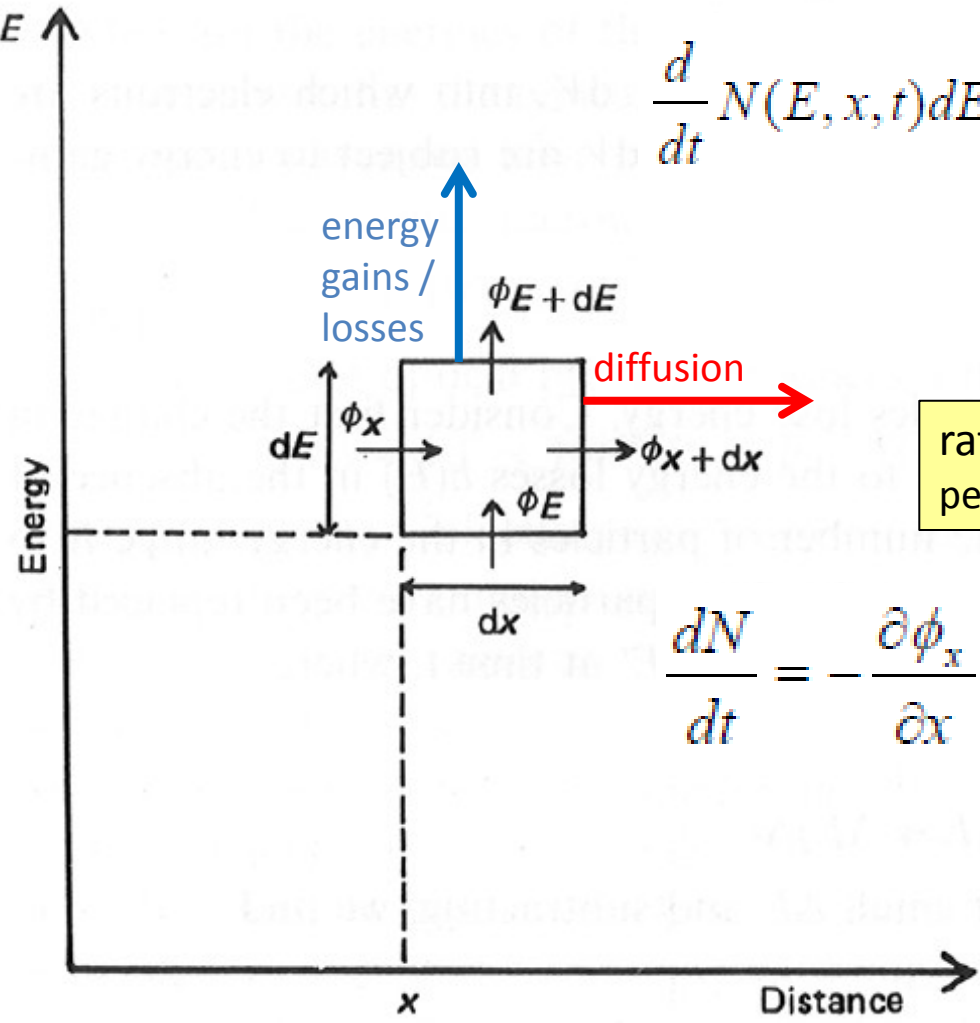
$$\epsilon = \frac{1}{2} m_{\pi} c^2 \frac{1 + \beta \cos \theta}{\sqrt{1 - \beta^2}}$$



- Background photons:
 - CMB, IR (UV heating), soft thermal X-rays
- Acceleration @ shocks:
 - In relativistic winds (pulsars, young stars)
 - Shell-type SNRs
 - Pulsar magnetosphere
- Variability:
 - Fast in compact sources

Diffusion-Loss Equation





$$\frac{d}{dt} N(E, x, t) dE dx = [\phi_x(E, x, t) - \phi_{x+dx}(E, x + dx, t)] dE + [\phi_E(E, x, t) - \phi_{E+dE}(E + dE, x, t)] dx + Q(E, x, t) dE dx,$$

rate of particles production per unit volume of coord space

$$\frac{dN}{dt} = -\frac{\partial \phi_x}{\partial x} - \frac{\partial \phi_E}{\partial E} + Q$$

by definition: $\phi_x = -D \frac{\partial N}{\partial x}$

$$\implies \frac{dN}{dt} = D \frac{\partial^2 N}{\partial x^2} - \frac{\partial \phi_E}{\partial E} + Q$$

energy loss for particles of energy E

$$-dE/dt = b(E) \implies N(E) \frac{dE}{dt} = \phi_E = -b(E)N(E)$$

$$\frac{dN(E)}{dt} = \frac{d}{dE} [b(E)N(E)] + Q(E, t) + D \nabla^2 N(E)$$

Energy loss processes: protons

● Ionization losses

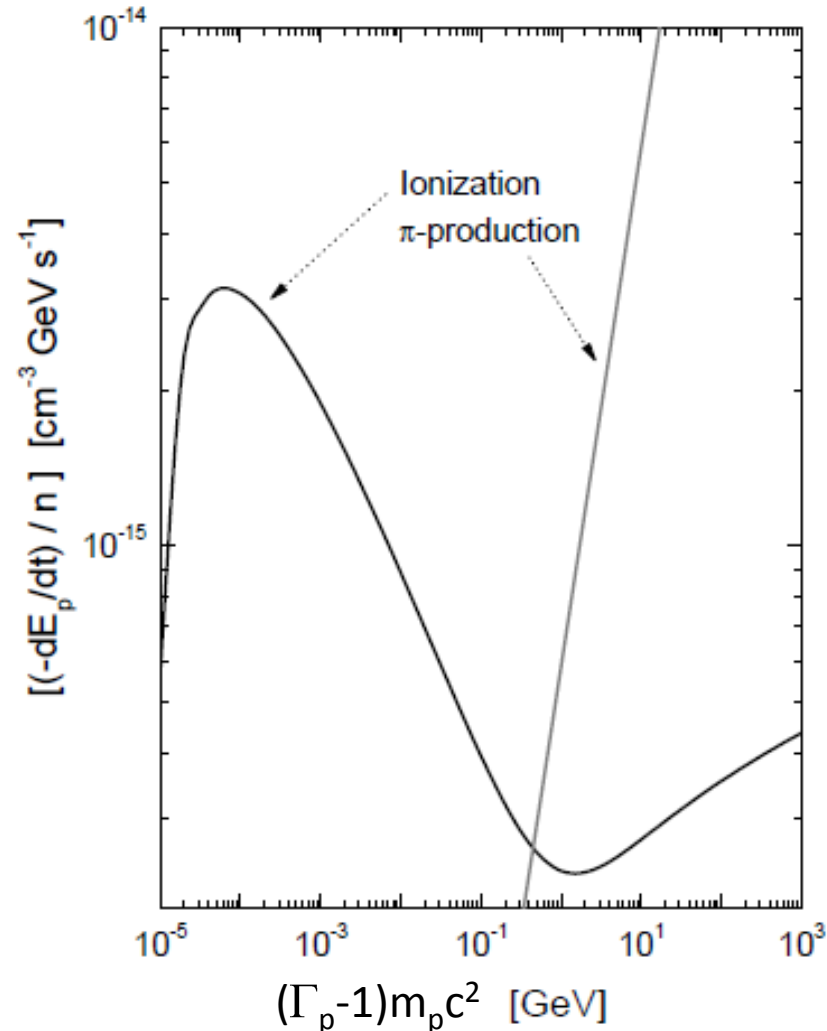
$$-\left(\frac{d\Gamma_p}{dt}\right)_{\text{Ion},p} \cong \begin{cases} 10^{-14} n_p (1-\Gamma_p^{-2})^{-1/2} [10.9 + 2 \ln \Gamma_p + \ln(1-\Gamma_p^{-2}) + (1-\Gamma_p^{-2})] & \text{s}^{-1} \\ 10^{-15} n_p [26.73 + 3 \ln(\Gamma_p)] & \text{s}^{-1} \end{cases}$$

$$\Gamma_p > 2000$$

● Pion production

$$-\left(\frac{d\Gamma_p}{dt}\right)_{\text{Pion},p} \cong 3.7 \times 10^{-13} n_p (\Gamma_p^{-1})$$

$$\Gamma_p > 2.38 \quad (\rightarrow 1.22 \text{ GeV})$$



Energy loss processes: electrons

$$b(\gamma) = b_{\text{Coul}}(\gamma) + b_{\text{syn}}(\gamma) + b_{\text{IC}}(\gamma) + b_{\text{brem}}(\gamma) + b_{\text{AW}}(\gamma)$$

- Coulomb interactions with thermal electrons

$$b_{\text{Coul}}(\gamma) \approx 1.2 \times 10^{-12} n_e \left[1.0 + \frac{\ln(\gamma/n_e)}{75} \right] \text{ s}^{-1}$$

- synchrotron radiation

$$b_{\text{syn}}(\gamma) = \frac{4}{3} \frac{\sigma_T}{m_e c} \gamma^2 U_B = 1.30 \times 10^{-21} \gamma^2 \left(\frac{B}{1 \mu\text{G}} \right)^2 \text{ s}^{-1}$$

- Inverse Compton (IC) scattering

$$b_{\text{IC}}(\gamma) = \frac{4}{3} \frac{\sigma_T}{m_e c} \gamma^2 U_r = 1.37 \times 10^{-20} \gamma^2 (1+z)^4 \text{ s}^{-1}$$

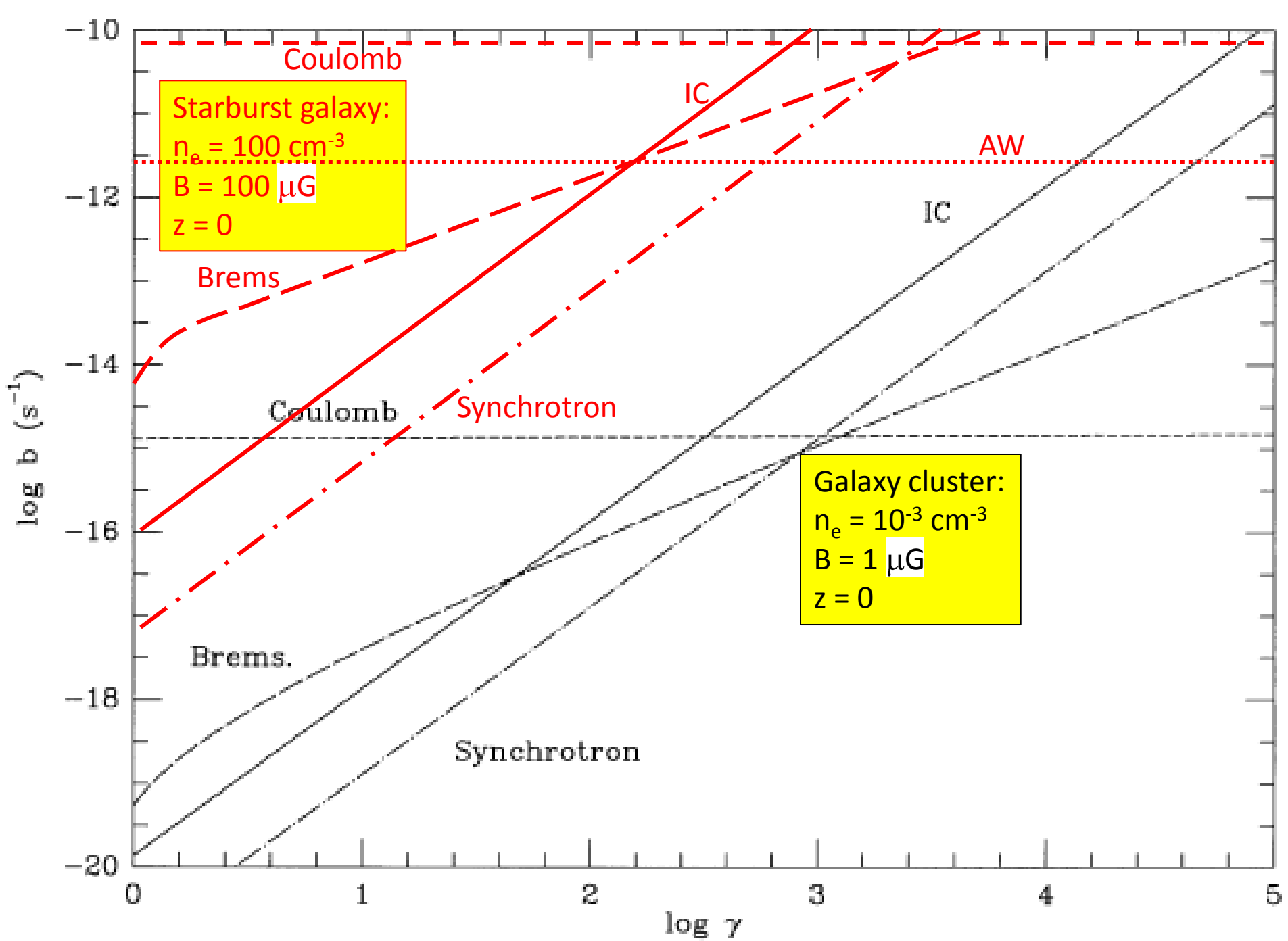
... for $U_r = 4 \times 10^{-13} \text{ erg cm}^{-3}$

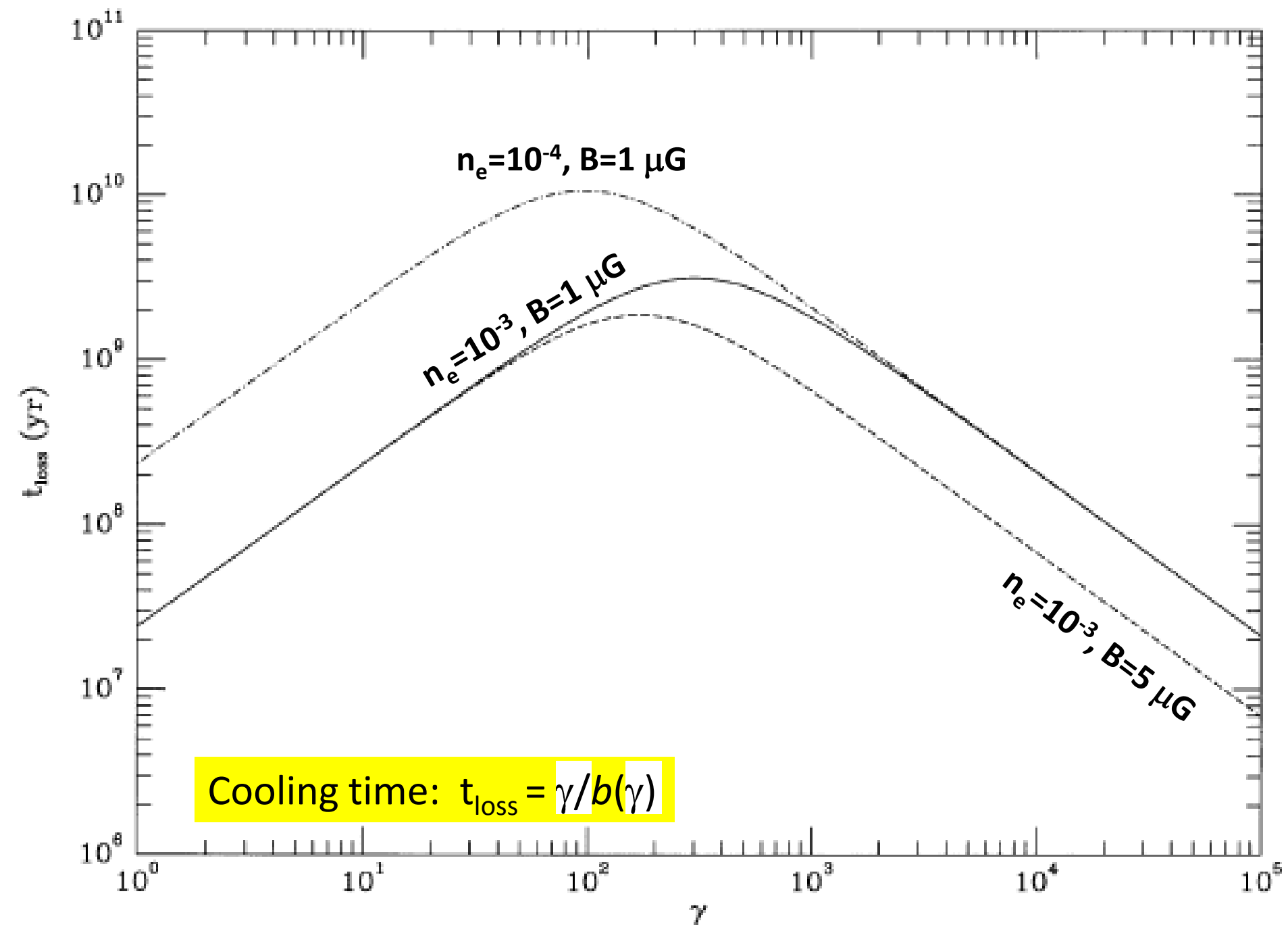
- bremsstrahlung radiation

$$b_{\text{brem}}(\gamma) \approx 1.51 \times 10^{-16} n_e \gamma [\ln(\gamma) + 0.36] \text{ s}^{-1}$$

- Scattering by Alfvén waves

$$b_{\text{AW}} = -B (4\pi\rho)^{-1/2} / L \gamma = 3 \times 10^{-16} (B/\mu\text{G}) n_e (L/0.3 \text{ kpc})^{-1} \gamma \text{ s}^{-1}$$





HE Gamma Rays in Galaxies

- electron spectrum

$$N_e(\gamma) = N_{e,0} \gamma^{-q} \quad \gamma_1 \leq \gamma \leq \gamma_2$$

- synchr. emissivity

$$F_\nu = 5.67 \times 10^{-22} (r_s^3/d^2) N_{e,0} a(q) B^{(q+1)/2} (\nu/4 \times 10^{16})^{-(q-1)/2} \text{ erg}/(\text{s cm}^2 \text{ Hz})$$

- electron spectrum: normalization, energy density

$$N_{e,0} = 5.72 \times 10^{-15} \psi a(q)^{-1} B^{-\frac{q+1}{2}} 250^{\frac{q-1}{2}}$$

$$\psi \equiv \left(\frac{r_s}{0.1 \text{ kpc}} \right)^{-3} \left(\frac{d}{\text{Mpc}} \right)^2 \left(\frac{f_{1 \text{ GHz}}}{\text{Jy}} \right)$$

$$U_e = N_{e,0} m_e c^2 \int_{\gamma_1}^{\gamma_2} \gamma^{1-q} d\gamma = 2.96 \times 10^{-22} 250^{\frac{q}{2}} \psi \frac{\gamma_1^{-q+2}}{(q-2) a(q)} B^{-\frac{q+1}{2}}$$

- particle/field energy density equipartition

$$U_p + U_e \simeq \frac{B^2}{8\pi}$$

• p/e energy density ratio

$$\kappa \equiv \frac{U_p}{U_e} = \frac{\int_{T_0}^{\infty} N_p(T) T dT}{\int_{T_0}^{\infty} N_e(T) T dT} = \frac{\left[\frac{T_0^2}{c^2} + 2T_0 m_p \right]^{\frac{q-1}{2}} \int_{T_0}^{\infty} T(T + m_p c^2) \left[\frac{T^2}{c^2} + 2T m_p \right]^{-\frac{q+1}{2}} dT}{\left[\frac{T_0^2}{c^2} + 2T_0 m_e \right]^{\frac{q-1}{2}} \int_{T_0}^{\infty} T(T + m_e c^2) \left[\frac{T^2}{c^2} + 2T m_e \right]^{-\frac{q+1}{2}} dT}$$

$T_0 =$
few keV

• p/e ratio

$$\frac{N_p(T)}{N_e(T)} \simeq \left(\frac{m_p}{m_e} \right)^{\frac{q-1}{2}} \left(\frac{T + m_p c^2}{T + m_e c^2} \right) \left(\frac{T + 2m_p c^2}{T + 2m_e c^2} \right)^{-\frac{q+1}{2}} \simeq \begin{cases} 1 & T \ll m_e c^2; \\ [T/(m_e c^2)]^{\frac{q-1}{2}} & m_e c^2 \ll T \ll m_p c^2 \\ \left(\frac{m_p}{m_e} \right)^{\frac{q-1}{2}} & m_p c^2 \ll T. \end{cases}$$

$\Rightarrow q=2.3 \rightarrow \kappa = U_p/U_e \approx 15 \quad N_p/N_e \big|_{>>1\text{GeV}} \approx 1.3 \times 10^2$

• equipartition magnetic field

$$B_{\text{eq}} = \left[7.46 \times 10^{-17} \frac{(2.5 \times 10^{-2})^{q/2}}{q-2} \psi \frac{1 + \kappa(q)}{a(q)} \right]^{\frac{2}{5+q}}$$

• CRp energy density

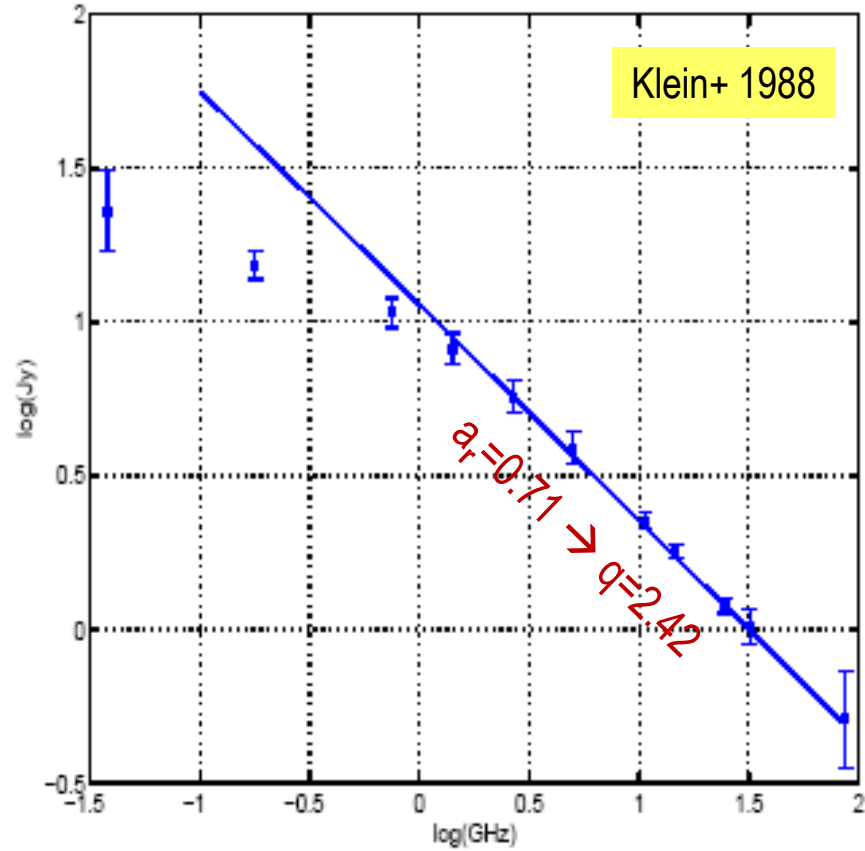
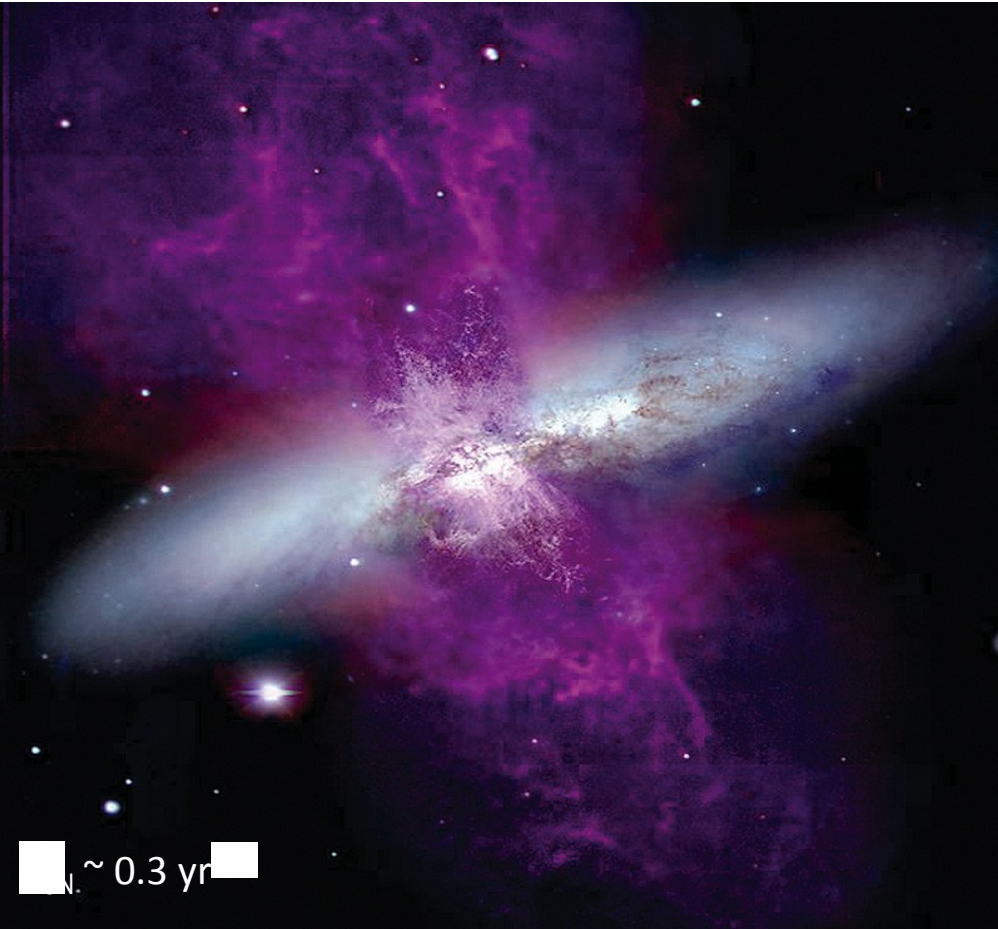
$$U_p = \frac{B^2}{8\pi (1 + \kappa^{-1})}$$

$$B_{\text{eq}} = \left\{ \frac{7.44 \times 10^{-21}}{1 + \chi} \left[1 + \frac{\kappa(q)}{1 + \chi} \right] \frac{\gamma_1^{2-q} 250^{q/2} \psi}{(q-2) a(q)} \right\}^{\frac{2}{5+q}}$$

$$U_p \left[1 + \frac{1 + \chi}{\kappa(q)} \right] \leftarrow \frac{B^2}{8\pi}$$

primary/secondary electron ratio ~ 0.5

M82 $d=3.6$ Mpc
 $r(\text{SB})=0.3$ kpc
 $f_{1\text{GHz}} = 10$ Jy



$L_{8-1000\mu\text{m}} = 2.2 \times 10^{44} \text{ erg s}^{-1} \rightarrow \text{SFR} \sim 10 M_{\odot} \text{ yr}^{-1}$

$B \simeq 95 \mu\text{G}$
 $N_{e,0} \simeq 10^{-4} \text{ cm}^{-3}$
 $U_e \simeq 20 \text{ eV cm}^{-3}$
 $U_p \simeq 200 \text{ eV cm}^{-3}$

(... M82 cont'd)

VHE γ -ray emission

analytical approx.

$$L(\geq \epsilon) = \int_V g(\geq \epsilon) n U_p dV \text{ s}^{-1}$$

SB nucleus: $r \leq 0.3 \text{ kpc}$

$$M_{H_2} = 2 \times 10^8 M_\odot$$

$$U_p = 200 \text{ eV cm}^{-3}$$

$$L_{>100\text{GeV}} = 1.6 \times 10^{39} \text{ s}^{-1} \rightarrow F_{>100\text{GeV}} = 10^{-12} \text{ cm}^{-2} \text{ s}^{-1}$$

External disk: $r > 0.3 \text{ kpc}$

Gas: flat, thin, exponential disk: $M_g = 2.5 \times 10^9 M_\odot$

$$U_n = 200 (R/R_{SB})^{-2}$$

$$L_{>100\text{GeV}} = 1.5 \times 10^{40} \text{ s}^{-1} \rightarrow F_{>100\text{GeV}} = 10^{-11} \text{ cm}^{-2} \text{ s}^{-1}$$

$$\Sigma(R) = \Sigma(0) e^{-R/R_d}$$

$$\Sigma(0) = 7.5 \text{E}+22 \text{ cm}^{-2}$$

$$R_d = 0.82 \text{ kpc}$$

α	$q_\gamma(\geq 100 \text{ MeV})$	$q_\gamma(\geq 1 \text{ TeV})$
4.1	0.46×10^{-13}	1.02×10^{-17}
4.2	0.58×10^{-13}	4.9×10^{-18}
4.3	0.61×10^{-13}	2.1×10^{-18}
4.4	0.57×10^{-13}	8.1×10^{-19}
4.5	0.51×10^{-13}	3.0×10^{-19}
4.6	0.44×10^{-13}	1.0×10^{-19}
4.7	0.39×10^{-13}	3.7×10^{-20}

Drury+
1994

Total flux: $F_{>100\text{GeV}} = 1.1 \times 10^{-11} \text{ cm}^{-2} \text{ s}^{-1}$

(... M82 cont'd)

numerical treatment
loss-propagation model

... same structure parameters

CR/field energy equip.
 p/e theoretically assumed

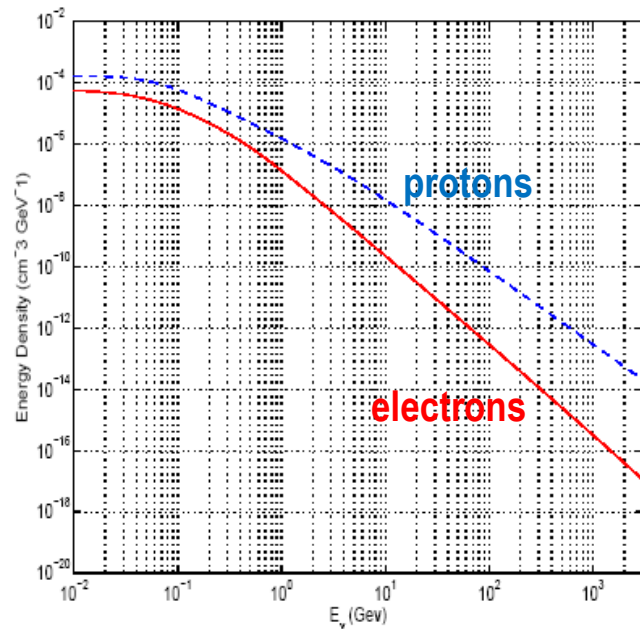
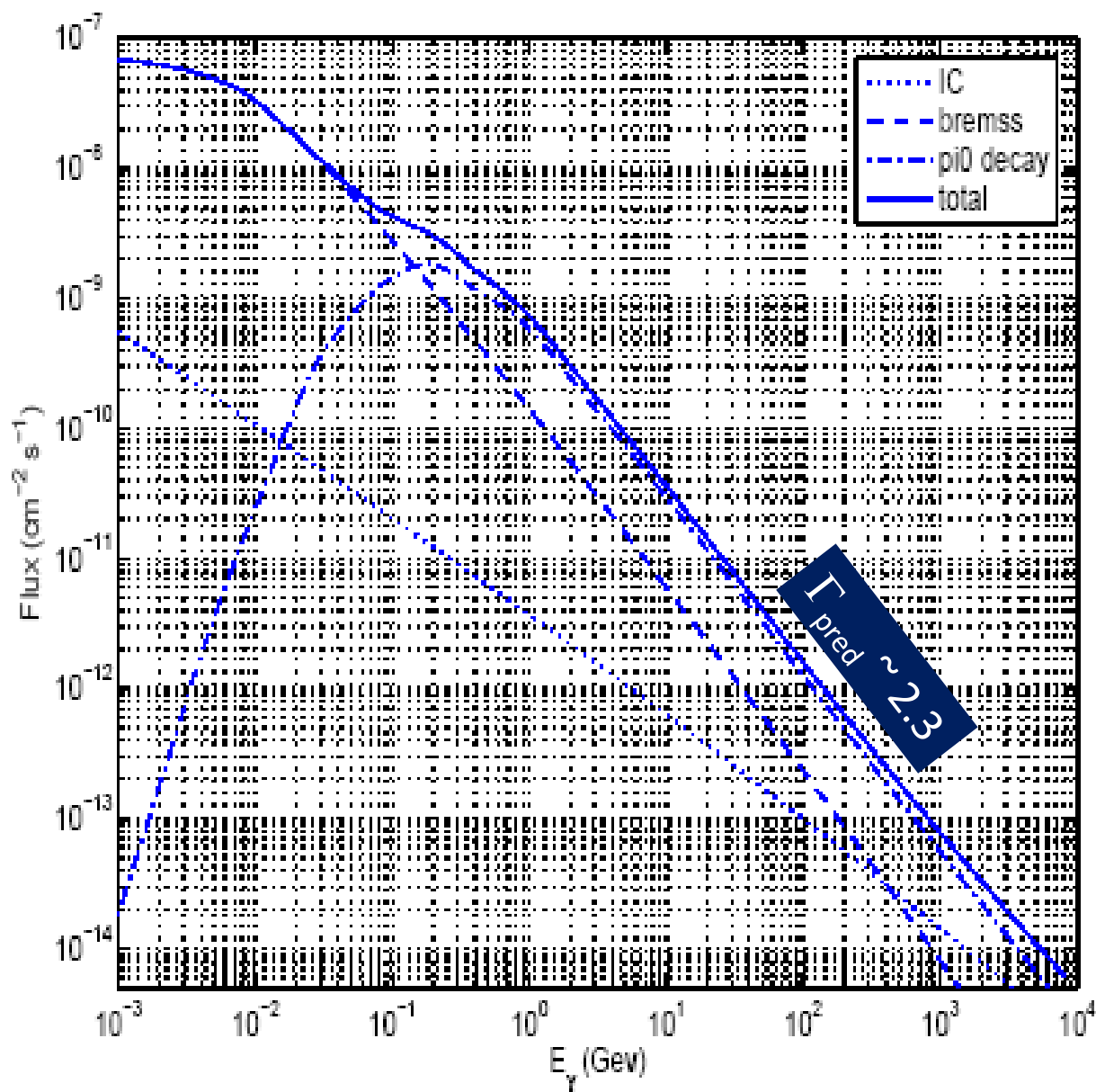
injection part. spectrum: $q=2$

... interactively \rightarrow

$$N_e \sim 10^{-4} \text{ cm}^{-3}$$

$$N_p/N_e (>>1 \text{ GeV}) \sim 50,$$

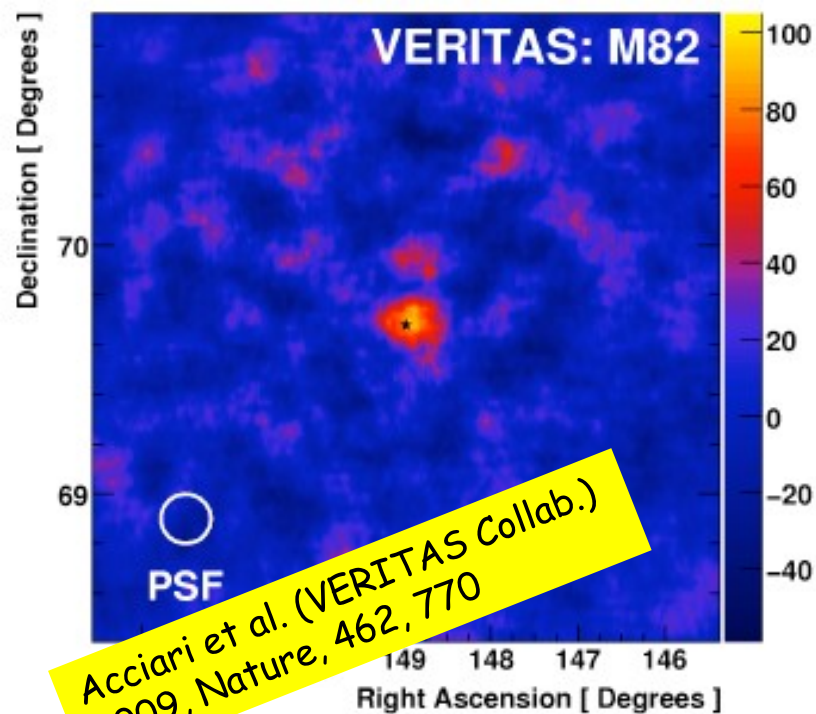
$$B_0 \sim 180 \mu\text{G}$$



$$F_{>100\text{MeV}} = E-8 \text{ cm}^{-2} \text{s}^{-1}$$

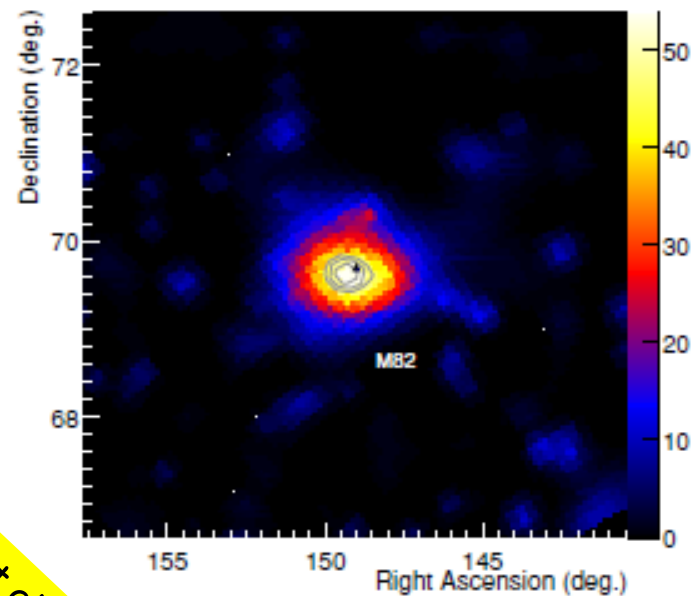
$$F_{>100\text{GeV}} = 2.5E-12 \text{ cm}^{-2} \text{s}^{-1}$$

$\geq 1/2$ sens. of MAGIC-II, VERITAS



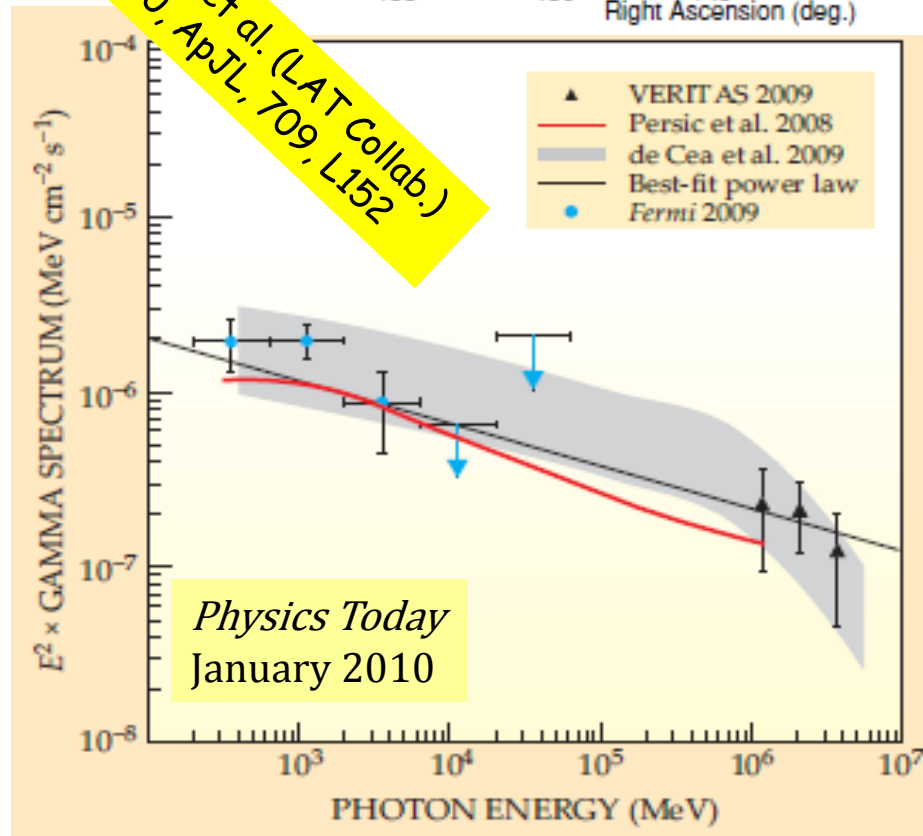
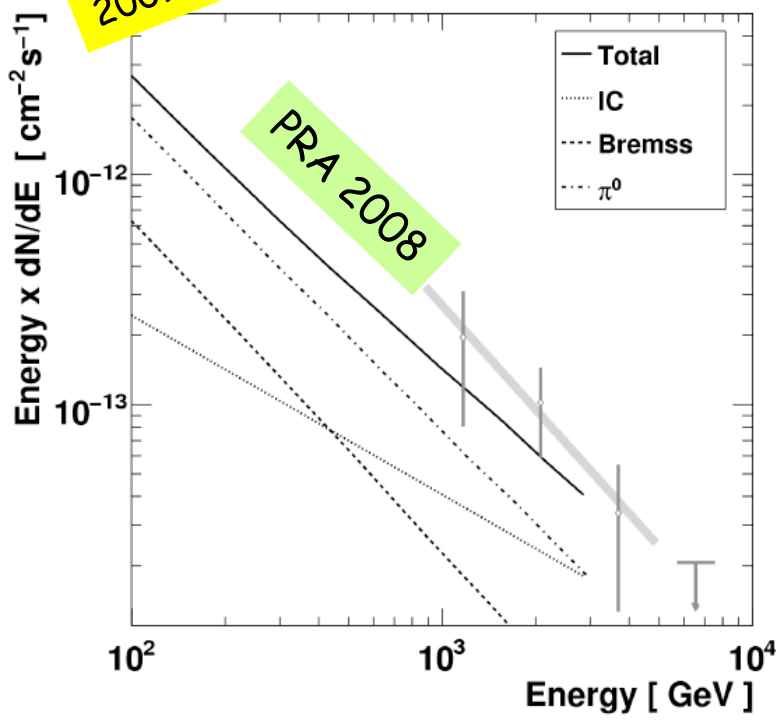
(... M82 cont'd)

**M82
detection**



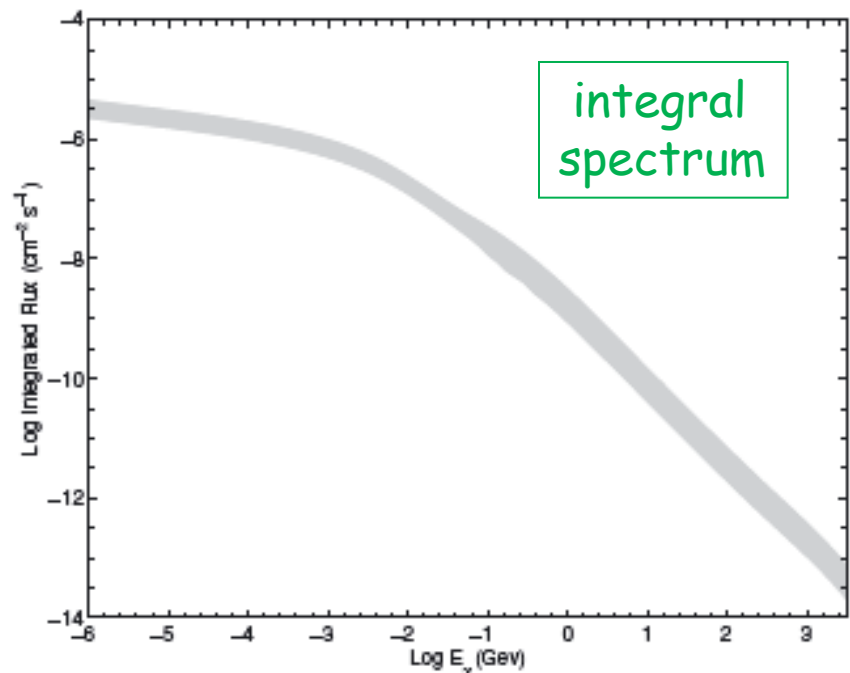
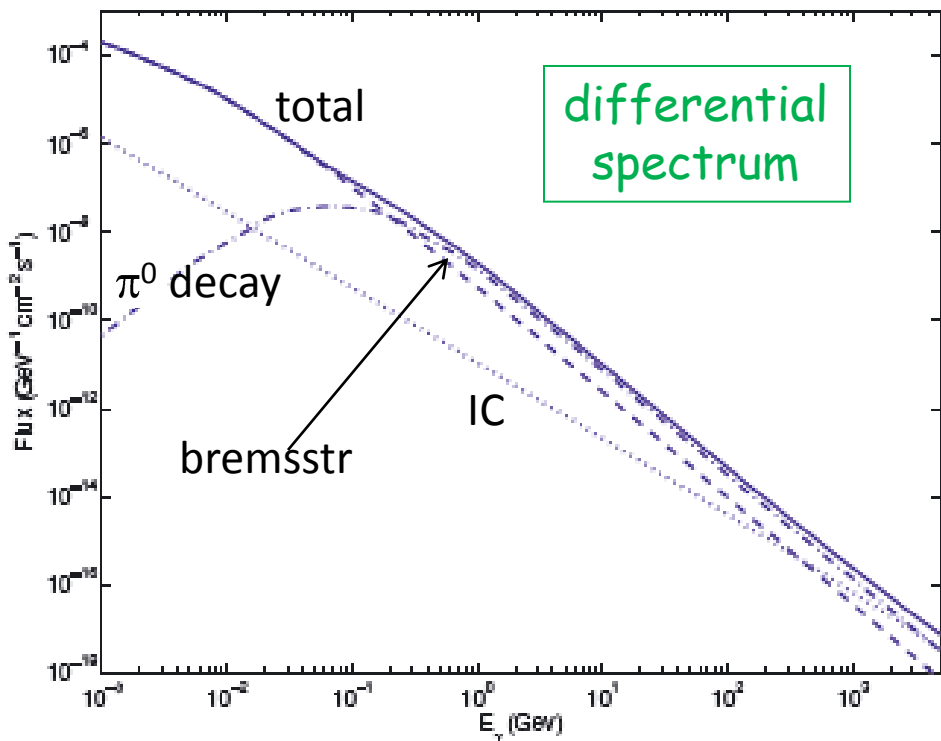
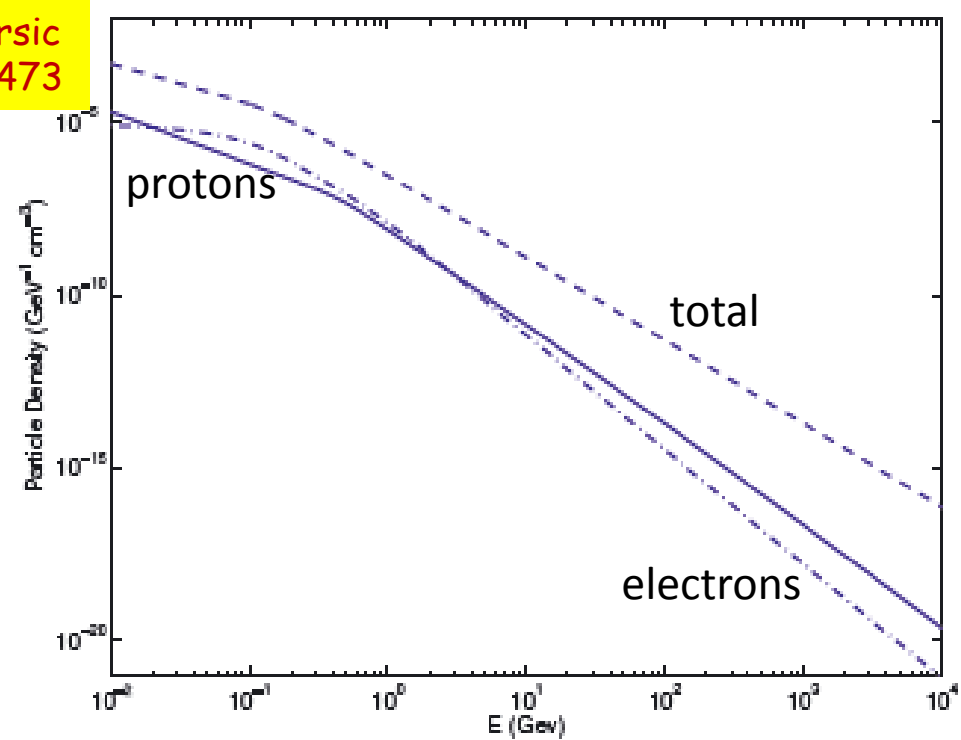
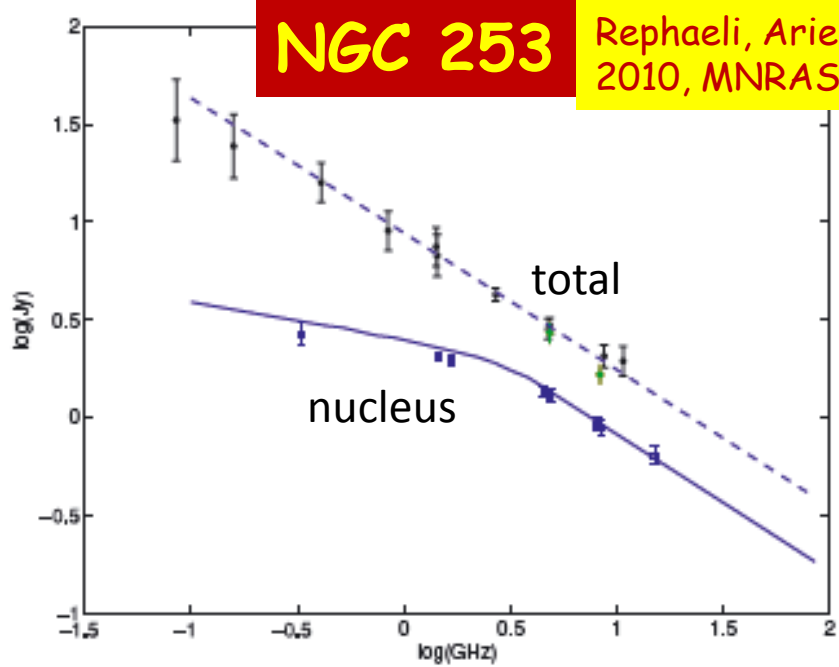
Acciari et al. (VERITAS Collab.)
2009, Nature, 462, 770

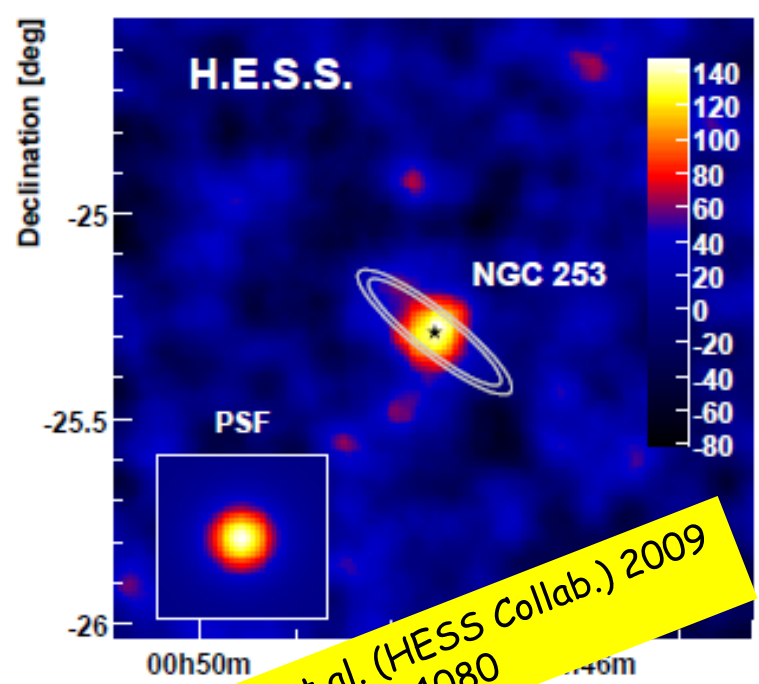
Abdo et al. (LAT Collab.)
2010, ApJL, 709, L152



NGC 253

Rephaeli, Arieli & Persic
2010, MNRAS, 401, 473

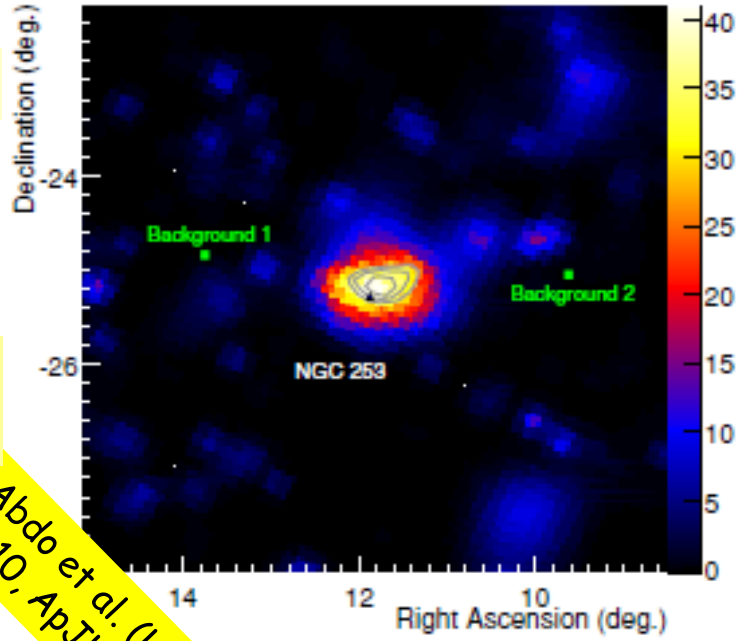




(... NGC253 cont'd)

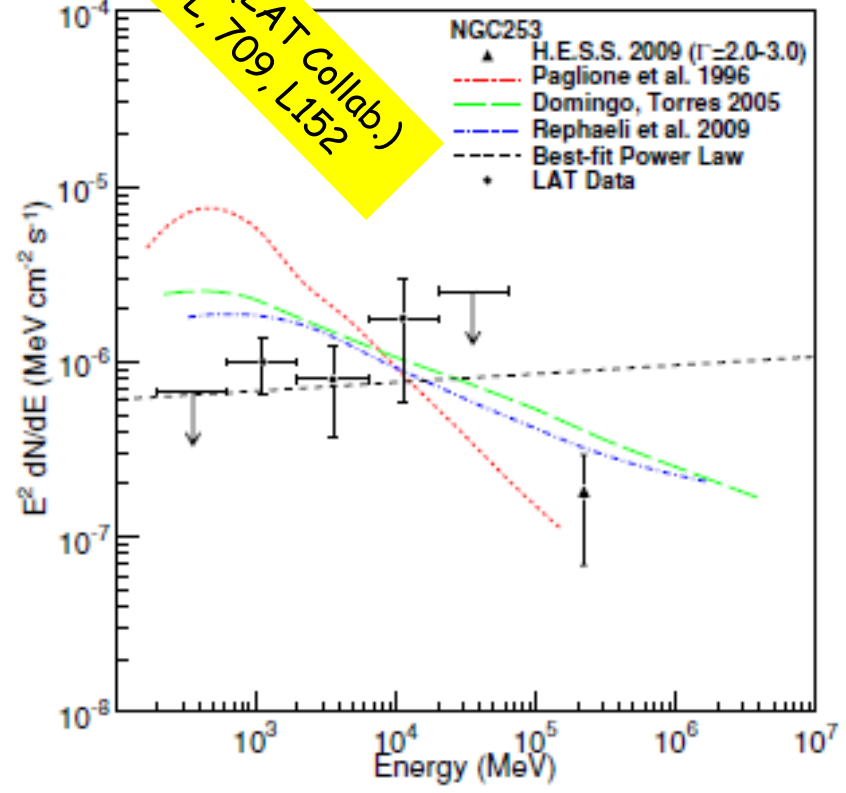
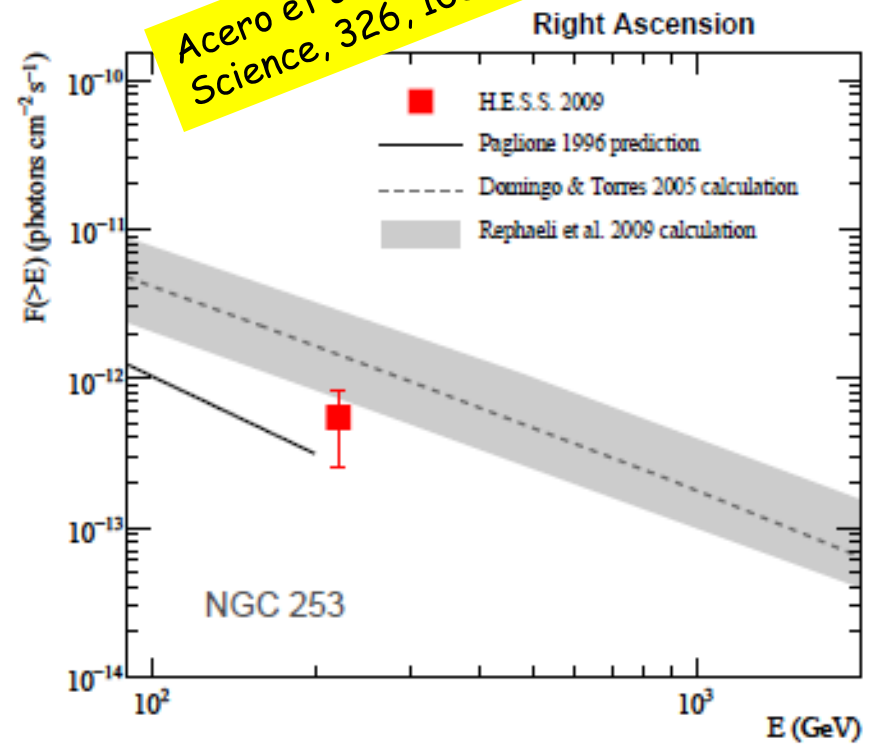
**NGC 253
detection**

$U_p \sim 150 \text{ eV cm}^{-3}$
in SB nucleus



Acero et al. (HESS Collab.) 2009
Science, 326, 1080

Abdo et al. (LAT Collab.)
2010, ApJL, 709, L152

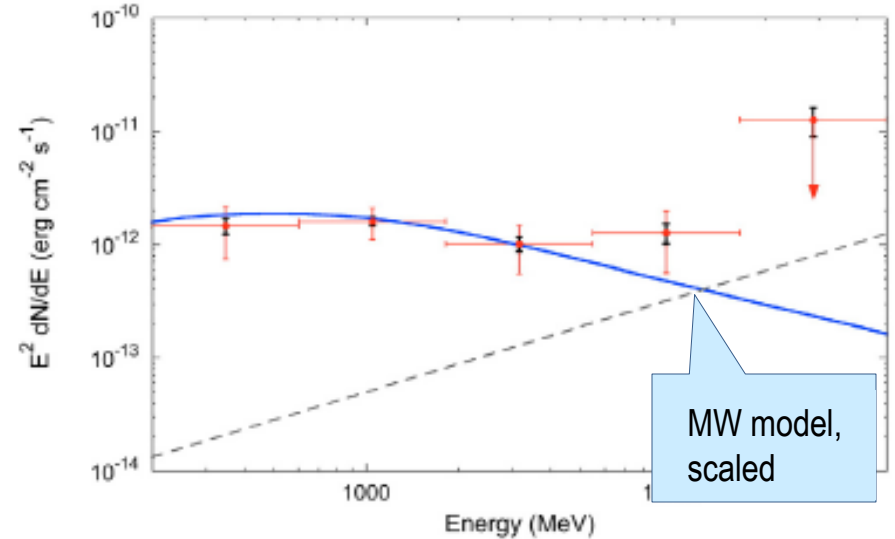
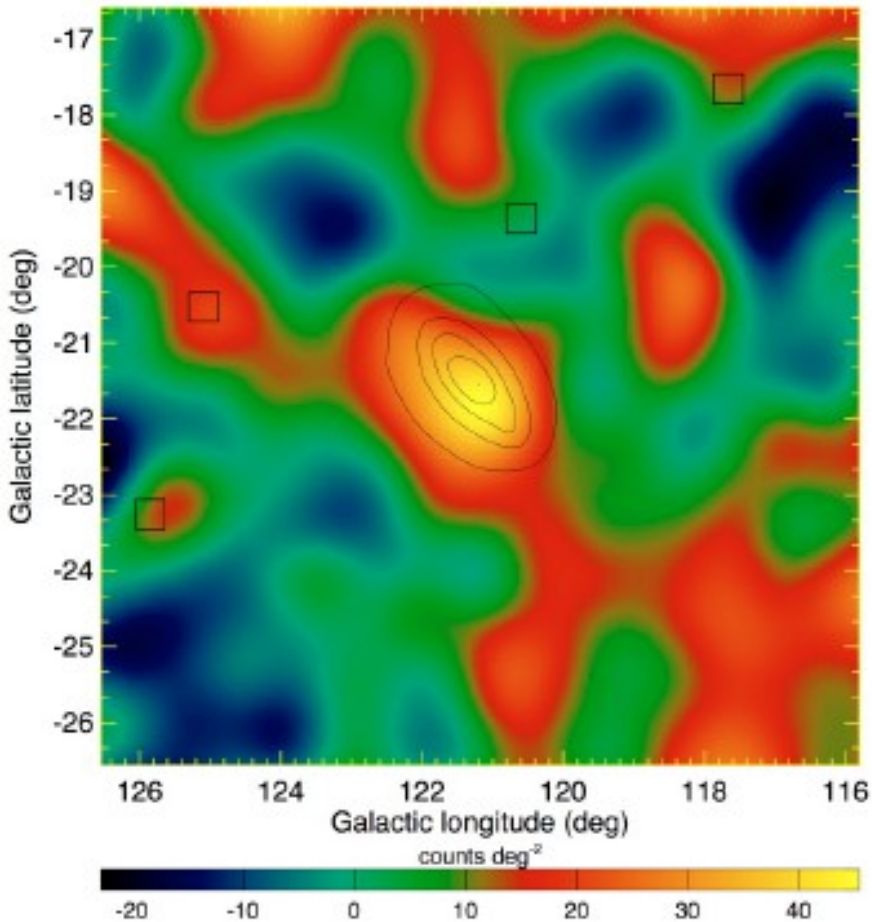


2. U_p from γ -rays

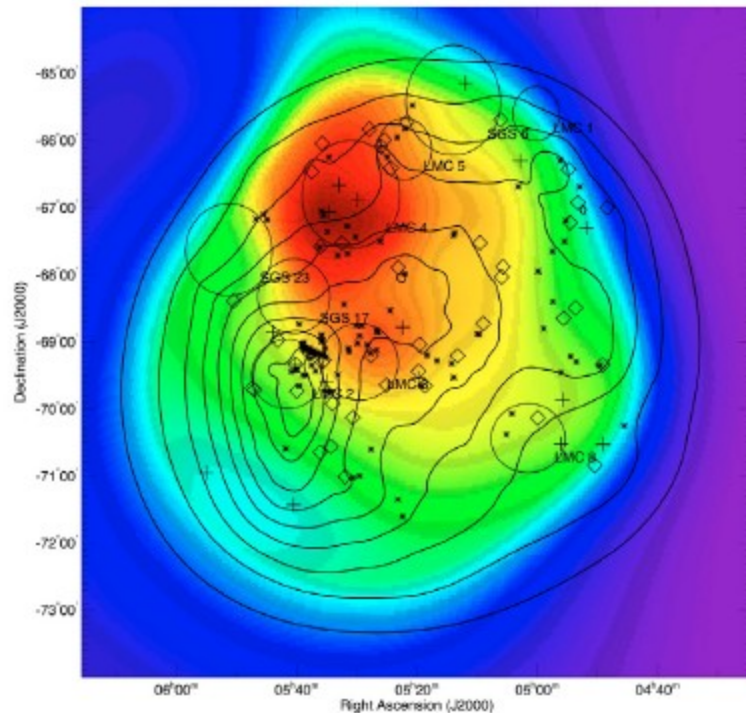
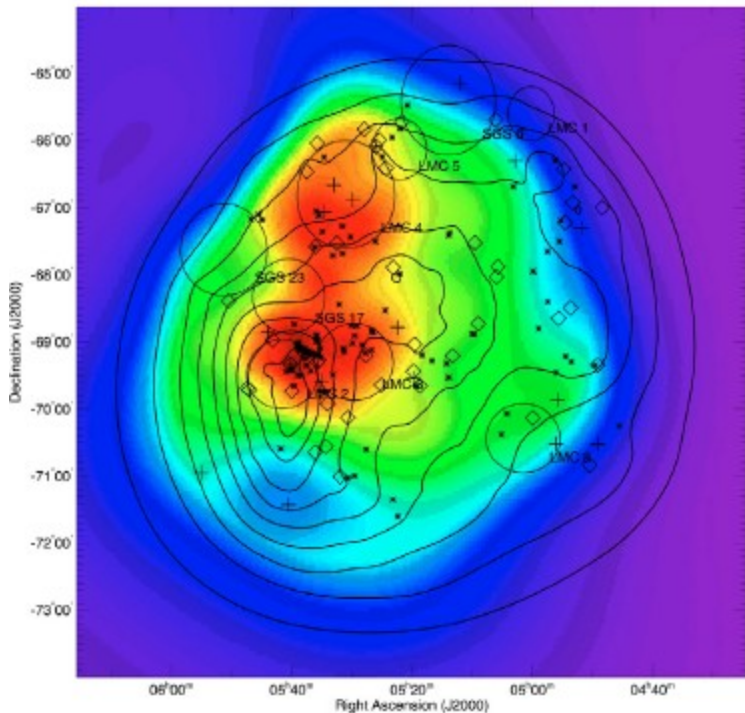
M31 (Andromeda Galaxy)

Abdo et al. (LAT Collab.)
2010, A&A, 523, L2

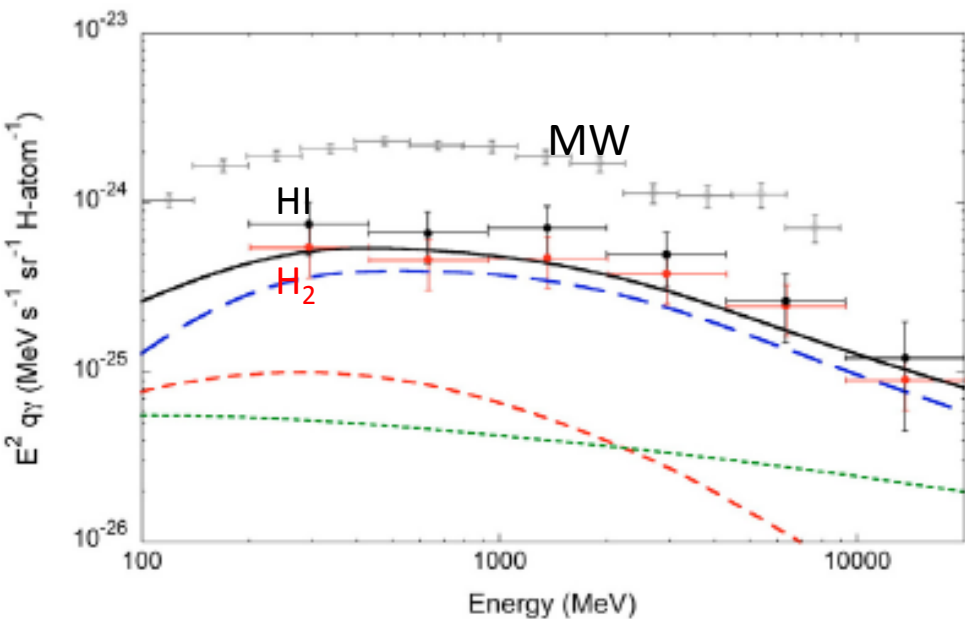
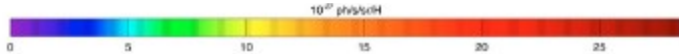
Galaxy	d kpc	M_{HI} $10^8 M_{\odot}$	M_{H_2} $10^8 M_{\odot}$	SFR $M_{\odot} \text{ yr}^{-1}$	F_{γ} $10^{-8} \text{ ph cm}^{-2} \text{ s}^{-1}$	L_{γ} $10^{41} \text{ ph s}^{-1}$
MW	...	$35 \pm 4^{(7)}$	$14 \pm 2^{(7)}$	$1-3^{(19)}$...	$11.8 \pm 3.4^{(28)}$
M31	$780 \pm 33^{(1)}$	$73 \pm 22^{(8)}$	$3.6 \pm 1.8^{(14)}$	$0.35-1^{(19)}$	0.9 ± 0.2	6.6 ± 1.4



$$U_p \sim 0.36 \text{ eV cm}^{-3}$$



Integrated >100 MeV emissivity maps of the LMC in units of 10^{-27} $\text{ph s}^{-1} \text{sr}^{-1} \text{H-atom}^{-1}$ for \mathcal{H}_1 (left panel) and \mathcal{H}_2 (right panel).



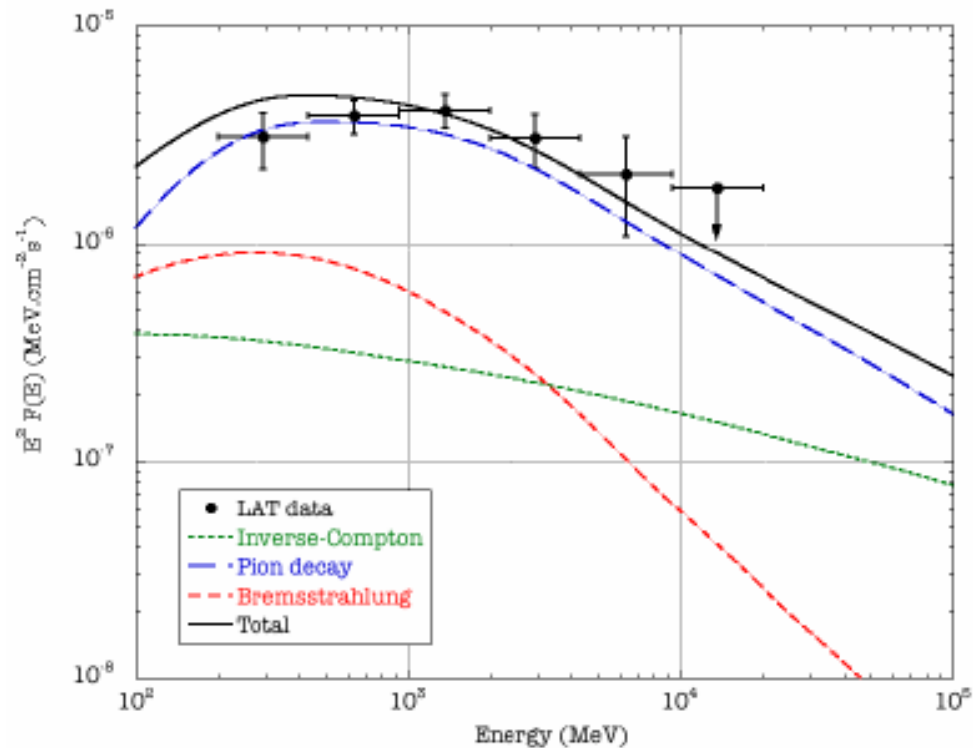
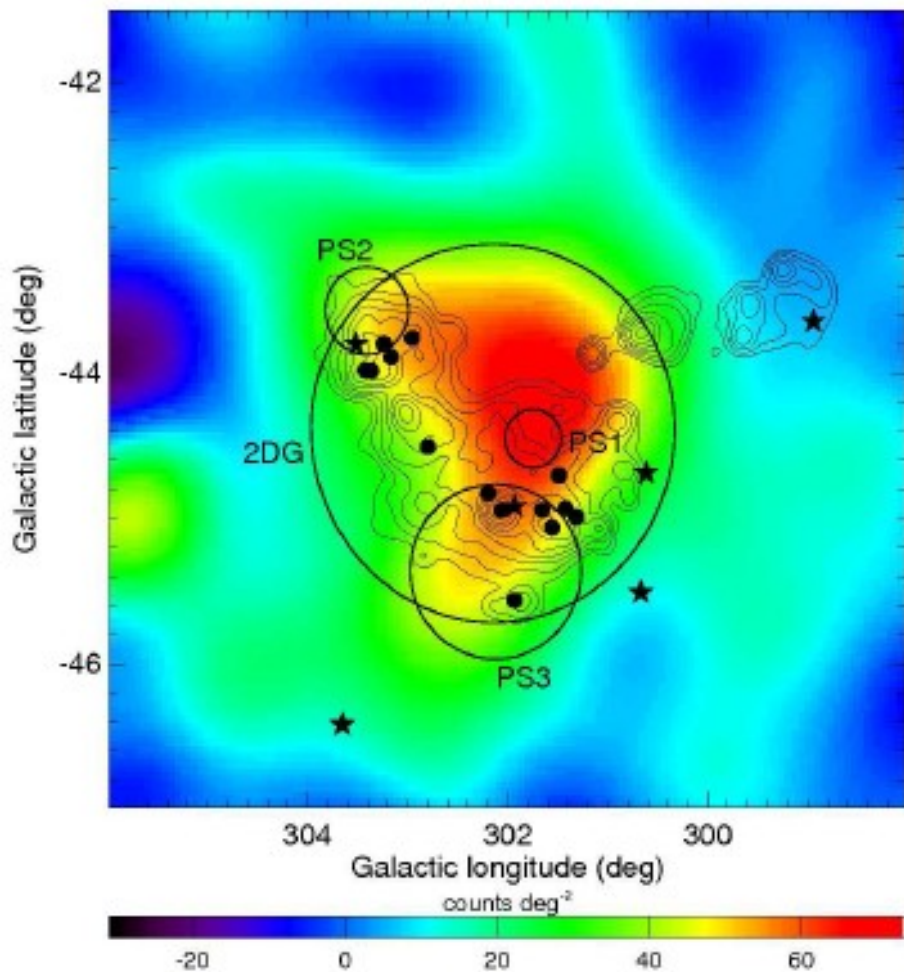
Large Magellanic Cloud (LMC)

Abdo et al. (LAT Collab.)
2010, A&A, 512, 7

$$U_p \sim 0.2-0.3 \text{ eV cm}^{-3}$$

Small Magellanic Cloud (SMC)

Abdo et al. (LAT Collab.)
2010, A&A, 523, A46



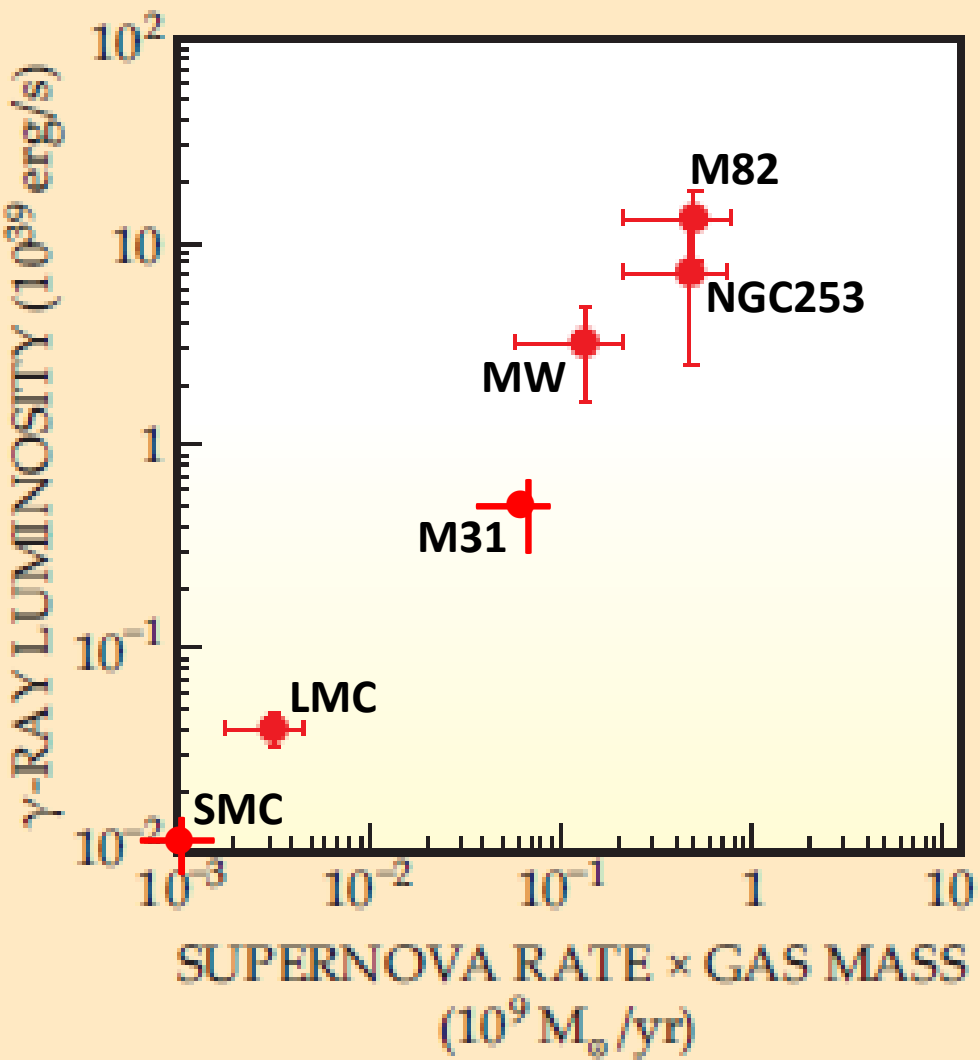
$$U_p \sim 0.15 \text{ eV cm}^{-3}$$

Adapted from:

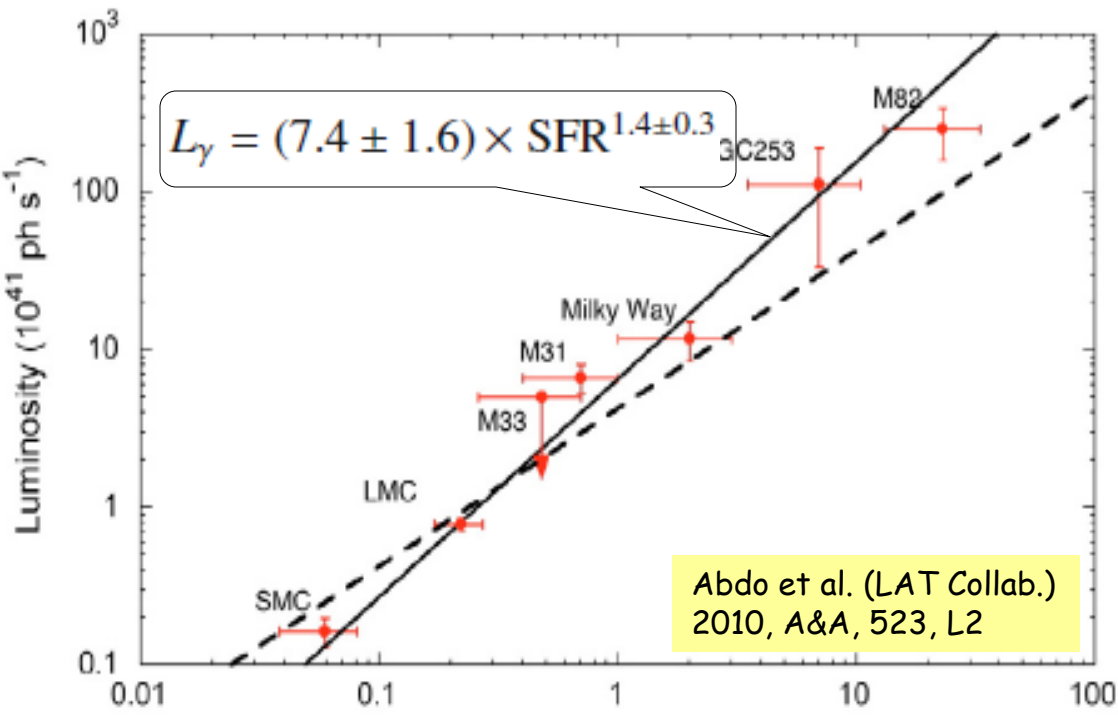
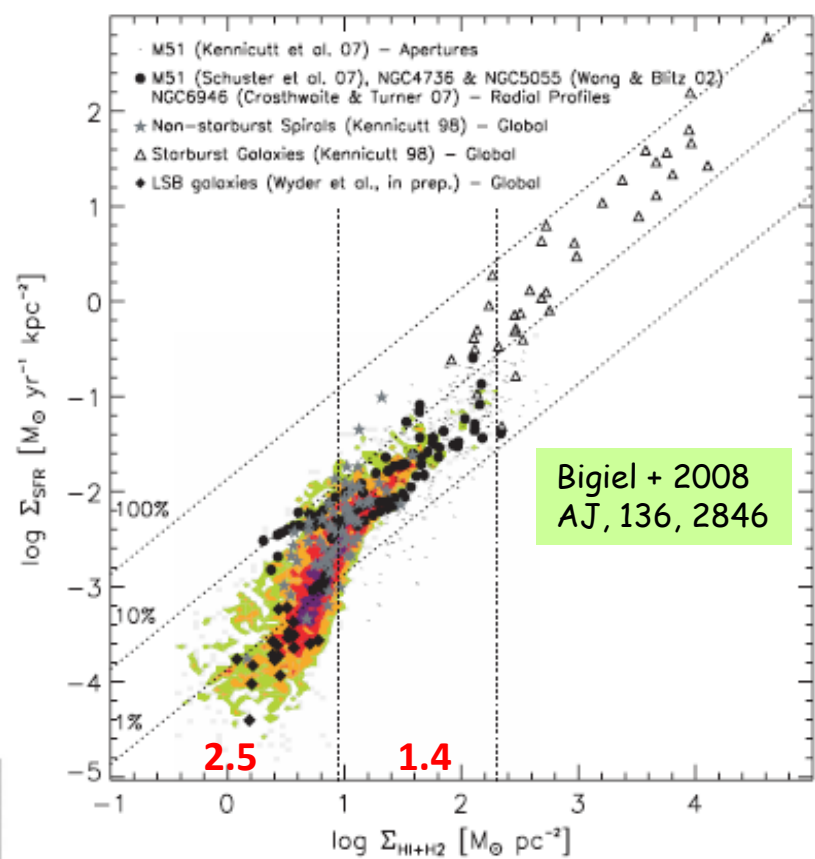
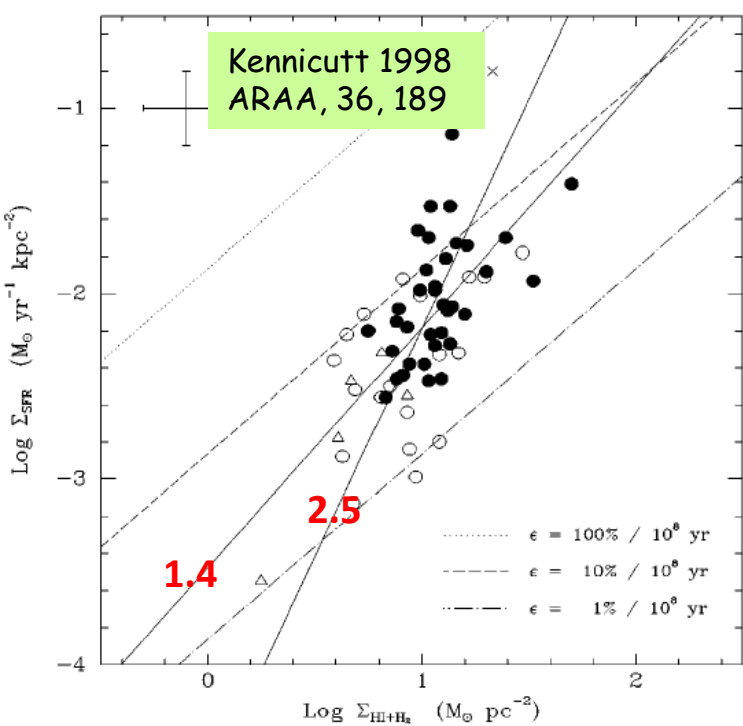
- Abdo et al. (LAT Collab.) 2010, ApJL, 709, L152;
- *Physics Today* (Jan. 2010)

$$L_{\gamma}^{(\geq \epsilon)} = \int_V g_{\gamma}^{(\geq \epsilon)} n U_P dV \text{ s}^{-1}$$

$\propto v_{SN} / r_s^3$
 $\sim \text{const, galaxy-wide}$
 M_H



HE emission from star-forming galaxies is mostly hadronic



Schmidt-Kennicutt SF law:

$$\Sigma_{\text{SFR}} \propto \Sigma_{\text{HI}+\text{H}_2}^\alpha$$

$$\alpha \sim 2.5$$

$$\rightarrow L_\nu \propto v_{\text{SN}} M_{\text{H}} \propto$$

$$\text{SFR } M_{\text{H}} \propto$$

$$\text{SFR}^{(1+1/\alpha)} = \text{SFR}^{1.4}$$

Measuring CR energy densities (U_p) in galaxies

① U_p from γ -ray emission: $L_{\geq \epsilon} = \int_V g_{\geq \epsilon} n U_p dV \quad \text{s}^{-1}$

Lifetime for energy gain: $\tau_+ = E/\dot{E} = (\Delta E/E)^{-1} \Delta t = \beta^{-1} \Delta t \sim 10^5 \text{ yr}$

Residency lifetime: $\tau_-^{-1} = \tau_{\text{out}}^{-1} + \tau_{\text{pp}}^{-1}$

M82: $\tau_{\text{out}} = 3 \times 10^4 \text{ yr}$

$$\tau_{\text{out}} = 3 \times 10^4 \left(\frac{r_s}{0.3 \text{ kpc}} \right) \left(\frac{v_{\text{out}}}{2500 \text{ km s}^{-1}} \right)^{-1} \text{ yr}$$

$$\tau_{\text{pp}} \sim 2 \times 10^7 n_p^{-1} \text{ yr}$$

M82: $\tau_{\text{pp}} = 2 \times 10^5 \text{ yr}$

Starburst lifetime: $\tau_{\text{SB}} \sim \tau_{\text{dyn}} \sim 10^8 \text{ yr}$

$\tau_+ \sim \tau_- \sim 10^5 \text{ yr} \ll \tau_{\text{SB}}$

Balance of gains vs losses achieved during SB

Equilibrium: min-energy configuration \rightarrow CR vs B equipartition

p/e ratio \rightarrow ② U_p from (radio synchrotron em. of) CRE

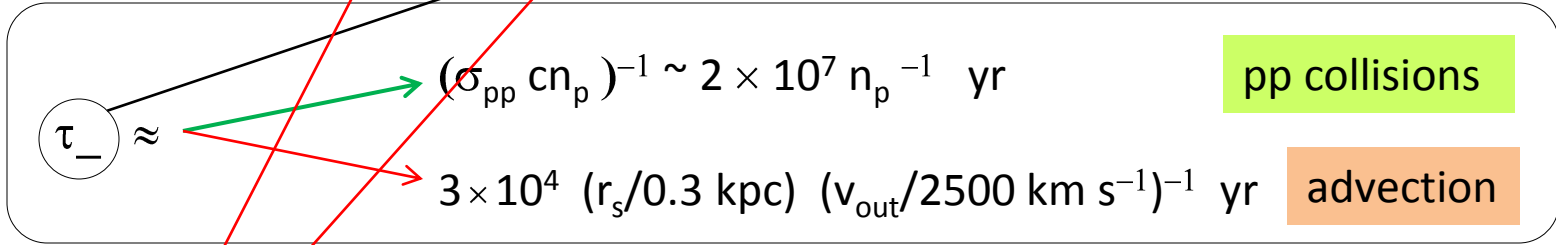
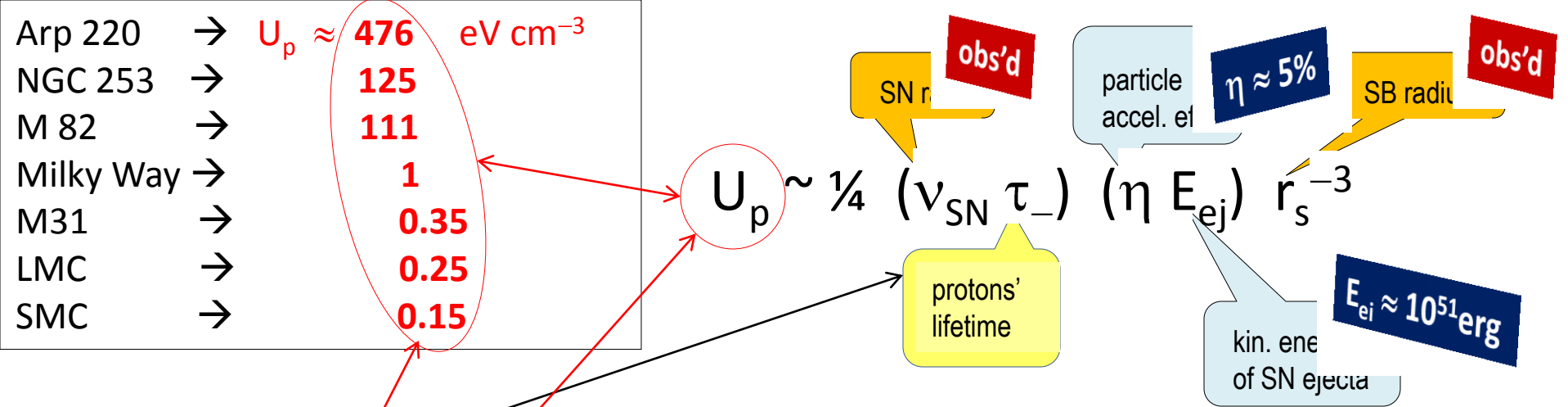
③ U_p from SN rate & residency time: $U_p \propto v_{\text{SN}} \tau_-$

Arp 220	→	$U_p \approx$	475	eV cm^{-3}	radio
NGC 253	→		125		radio, γ
M 82	→		111		radio, γ
Milky Way	→		1		...
M31	→		0.35		γ
LMC	→		0.25		γ
SMC	→		0.15		γ

U_p from supernovae

- ❖ massive star formation → SN
- ❖ SNR → Fermi-I mechanism → CR
- ❖ CR - SN relation (Ginzburg & Syrovatskii 1964)

$$U_p \sim \frac{1}{4} \overset{\text{observed}}{(v_{\text{SN}} \tau_-)} \overset{\text{Milky Way normalization}}{(\eta \epsilon_{\text{ej}})} \overset{\text{observed}}{r_s^{-3}}$$



$$U_p = 85 \frac{v_{SN}}{0.3 \text{ yr}^{-1}} \frac{\tau_-}{3 \times 10^4 \text{ yr}} \frac{\eta}{0.05} \frac{E_{ej}}{10^{51} \text{ erg}} \left(\frac{r_s}{0.3 \text{ kpc}}\right)^{-3} \text{ eV cm}^{-3}$$

Arp 220	515 eV cm ⁻³	3.50 yr ⁻¹	9.0E+3 yr <i>adv</i>	0.25 kpc
NGC 253	77 eV cm ⁻³	0.12 yr ⁻¹	2.0E+4 yr <i>adv</i>	0.20 kpc
M 82	95 eV cm ⁻³	0.25 yr ⁻¹	2.6E+3 yr <i>adv</i>	0.26 kpc
MW	1.8 eV cm ⁻³	0.02 yr ⁻¹	5.0E+6 yr <i>pp</i>	2.4 kpc
M31	0.7 eV cm ⁻³	0.01 yr ⁻¹	2.0E+7 yr <i>pp</i>	4.2 kpc
LMC	0.2 eV cm ⁻³	2 E-3 yr ⁻¹	1.0E+7 yr <i>pp</i>	3.0 kpc
SMC	1.0 eV cm ⁻³	1 E-3 yr ⁻¹	4.0E+7 yr <i>pp</i>	2.1 kpc

if CRp advected by diffusion $v_{diff}=100 \text{ km/s} \rightarrow U_p=0.15 \text{ eV/cm}^3$

CONCLUSIONS on CRs

U_p can be measured from:

- i) γ -ray emission (directly)
- ii) radio synchrotron emission (indirectly),
assuming p/e ratio, part./field equilibrium.
- iii) SN rates and CRp lifetimes.

Starbursts: $U_p \sim O(100) \text{ eV cm}^{-3}$

Quiet SFGs: $U_p \sim O(1) \text{ eV cm}^{-3}$

Universal(?) acceleration efficiency of SN.

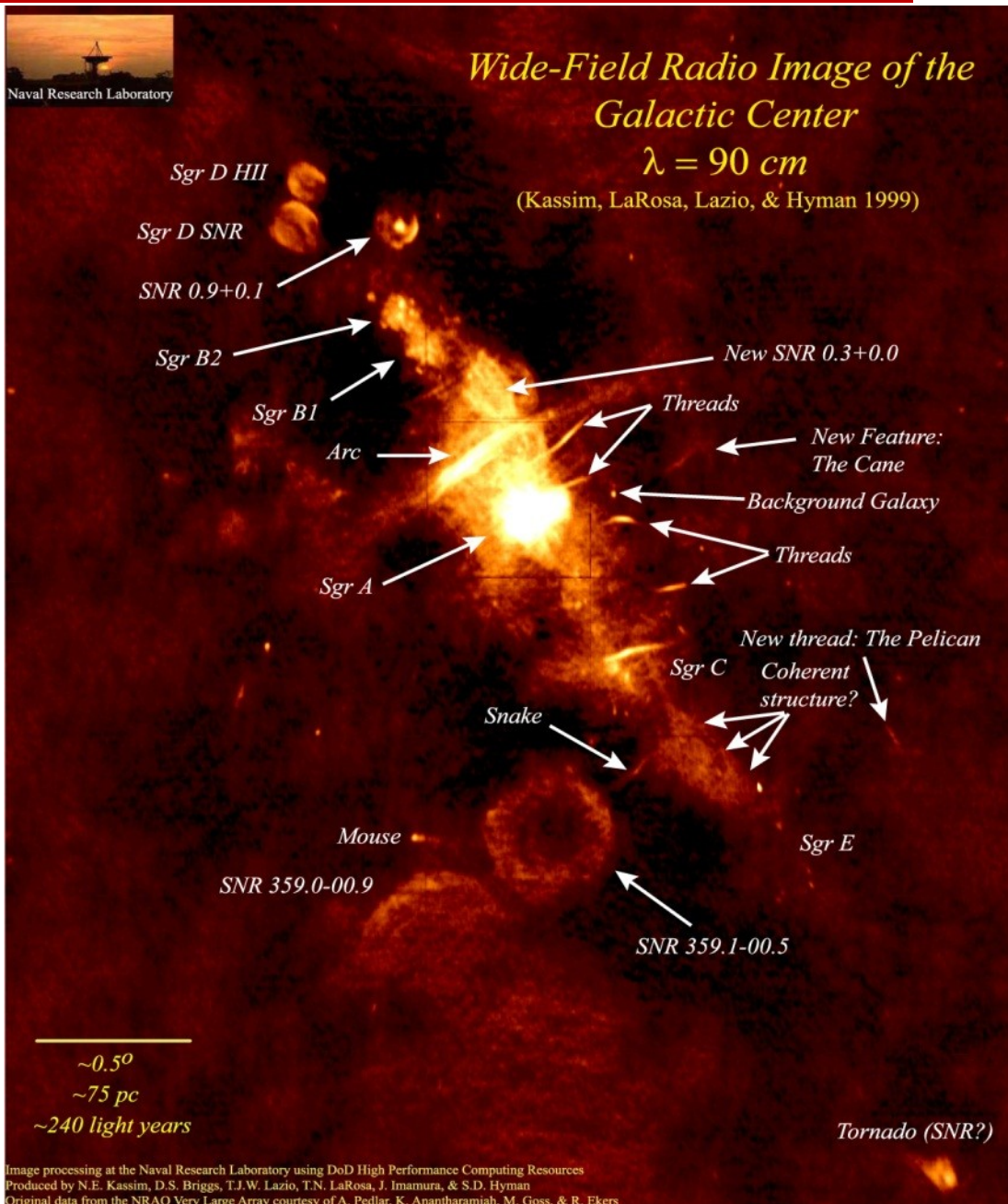
Fermi I acceleration at work (NR strong shock).

Particles/field equipartition in place.

→ radio data to study CRs in high-z SFGs

Happy ending?

Targets for DM search



Requirements:

1. Not associated with known conventional TeV sources
2. High DM density
3. Close by
4. Not extended

1. Galactic Center

Distance $\sim 7.5 \text{ kpc} \rightarrow \text{OK}$

... but:

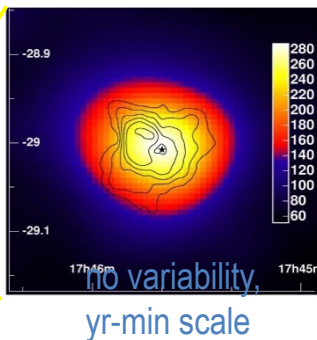
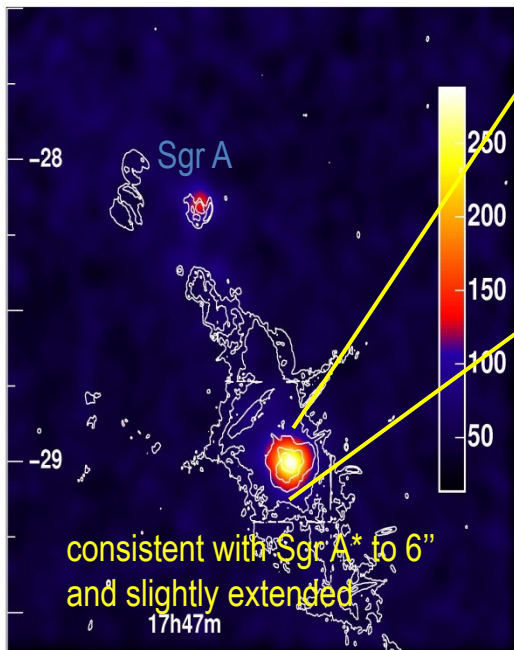
other γ -ray sources in the FOV,
i.e. SNR Sgr A East

\rightarrow plausible competing scenarios

2. Dwarf Sph galaxies

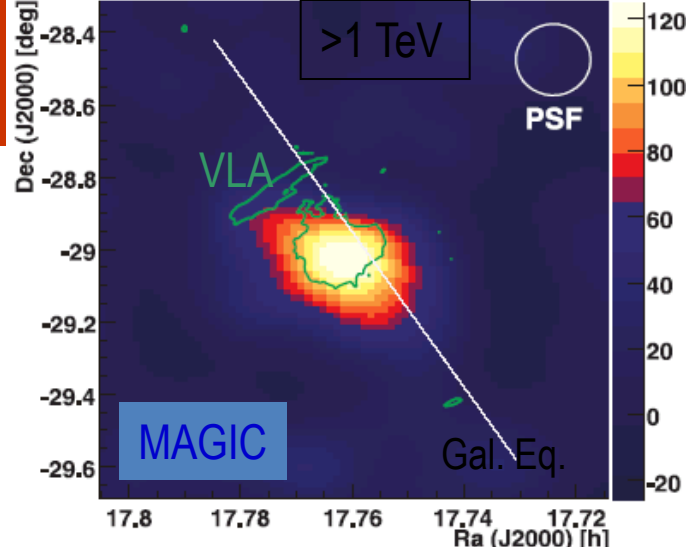
ok 1(?), 2, 3, 4

1. The Galactic Center



Detected: Cangaroo 2003
 Confirmed: HESS 2004
 Confirmed: MAGIC 2005

Diffuse GP emission revealed by subtracting strong sources
 Correlation with molecular gas
 CRs interacting with MCs
 GC source coincident w. Sgr A*



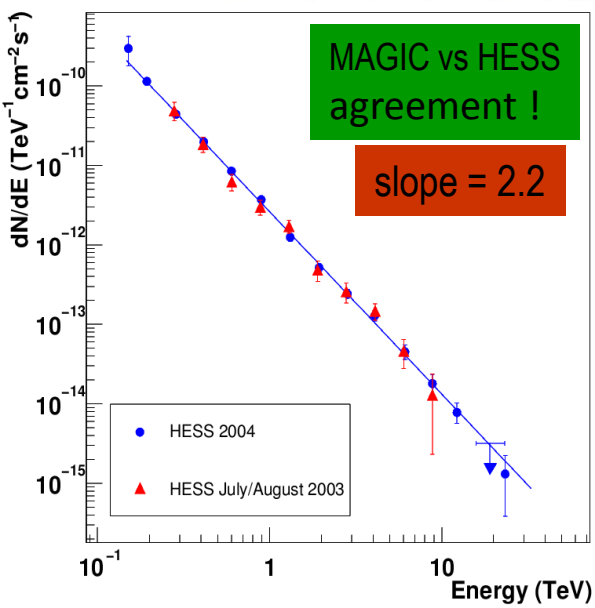
Supernova Remnant G0.9+0.1

HESS J1745-290 (The Galactic Centre)

Subtracted image

Emission along the Galactic Plane

Unidentified Source HESS J1745-303



GC signal: unlikely to be DM

Some background
on galaxy structure ..

$$I(r) = I_0 \exp(-r/R_d)$$

same profile at
all luminosities!

1000 galaxies
Persic + 1996

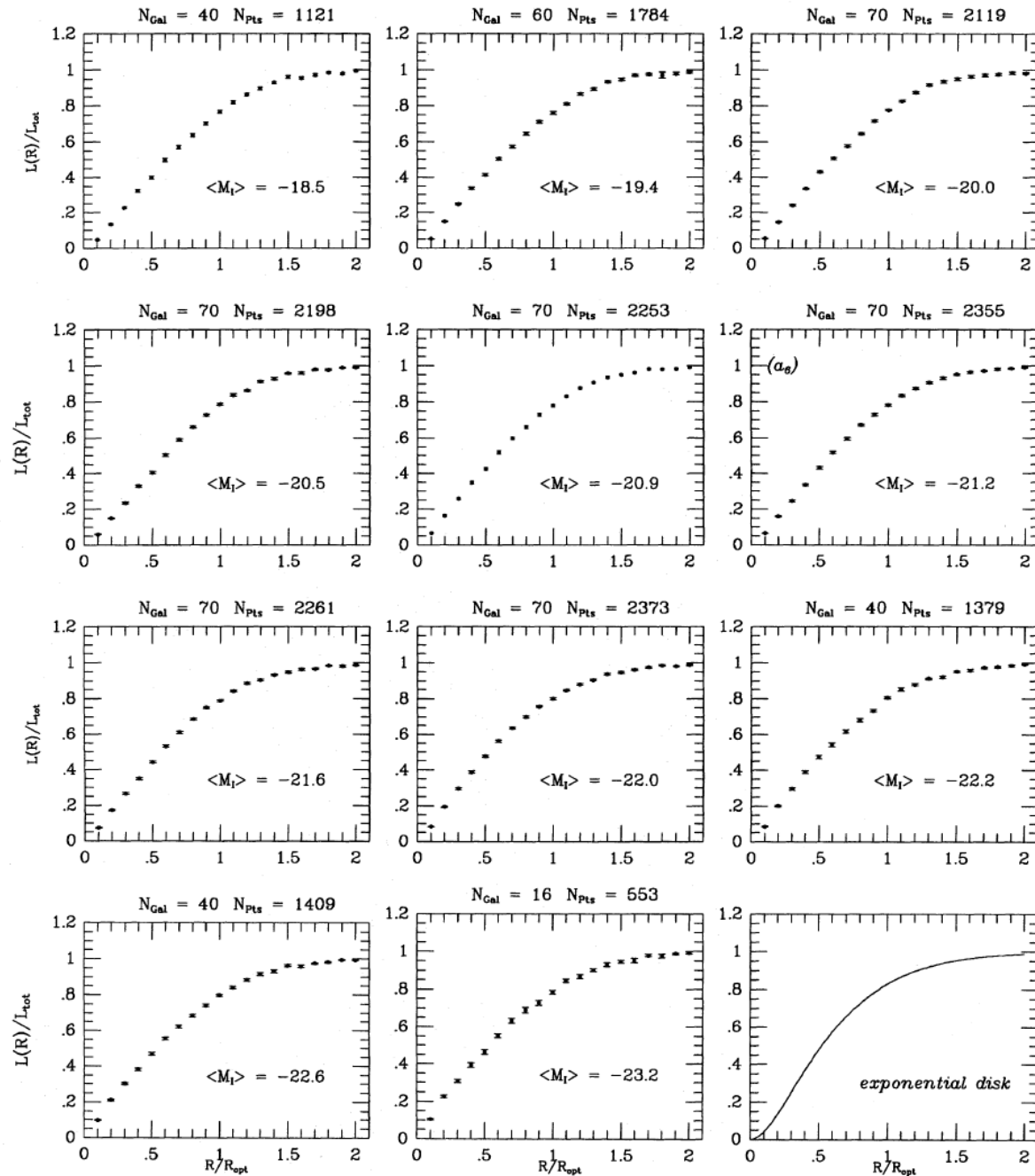
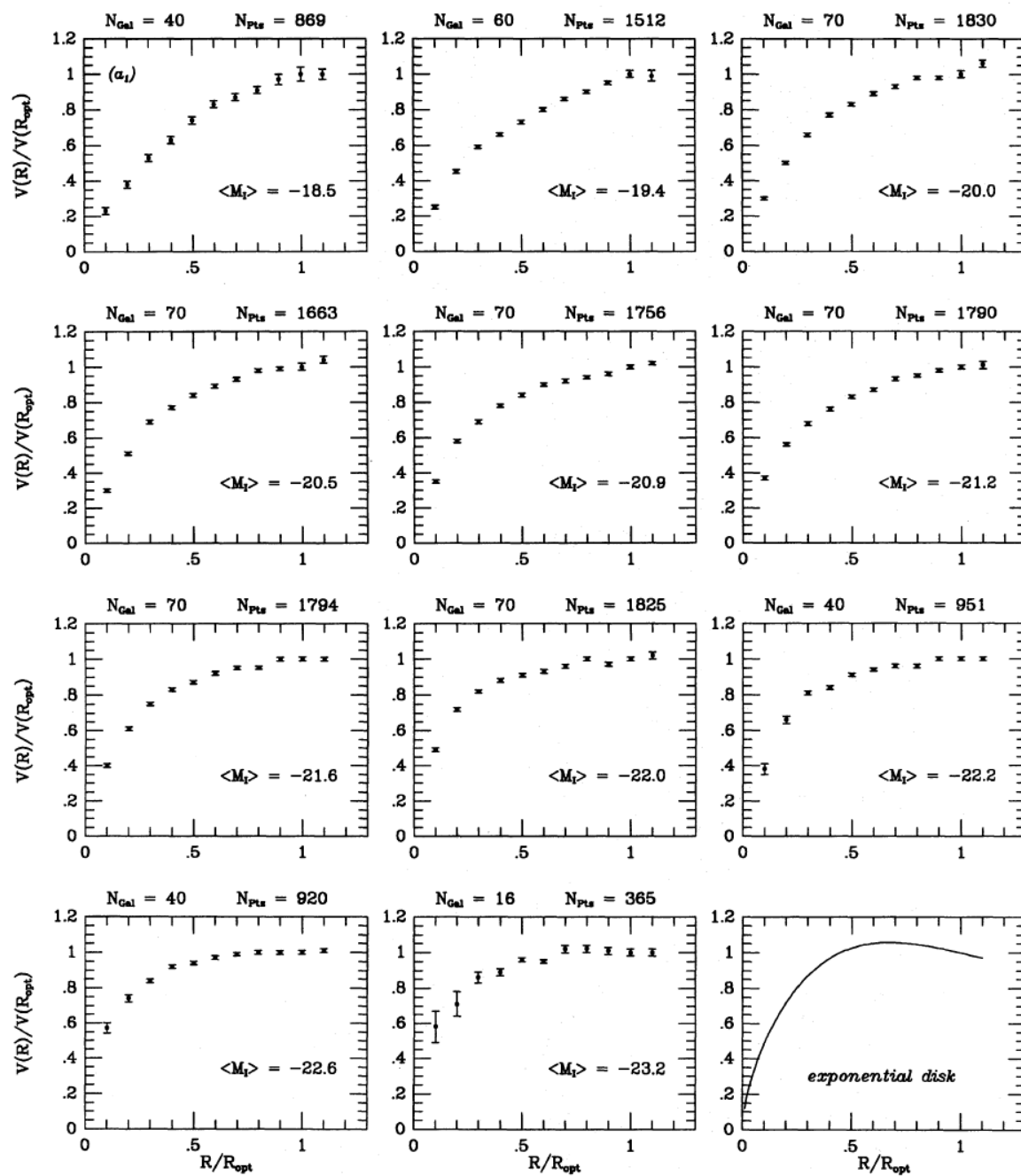
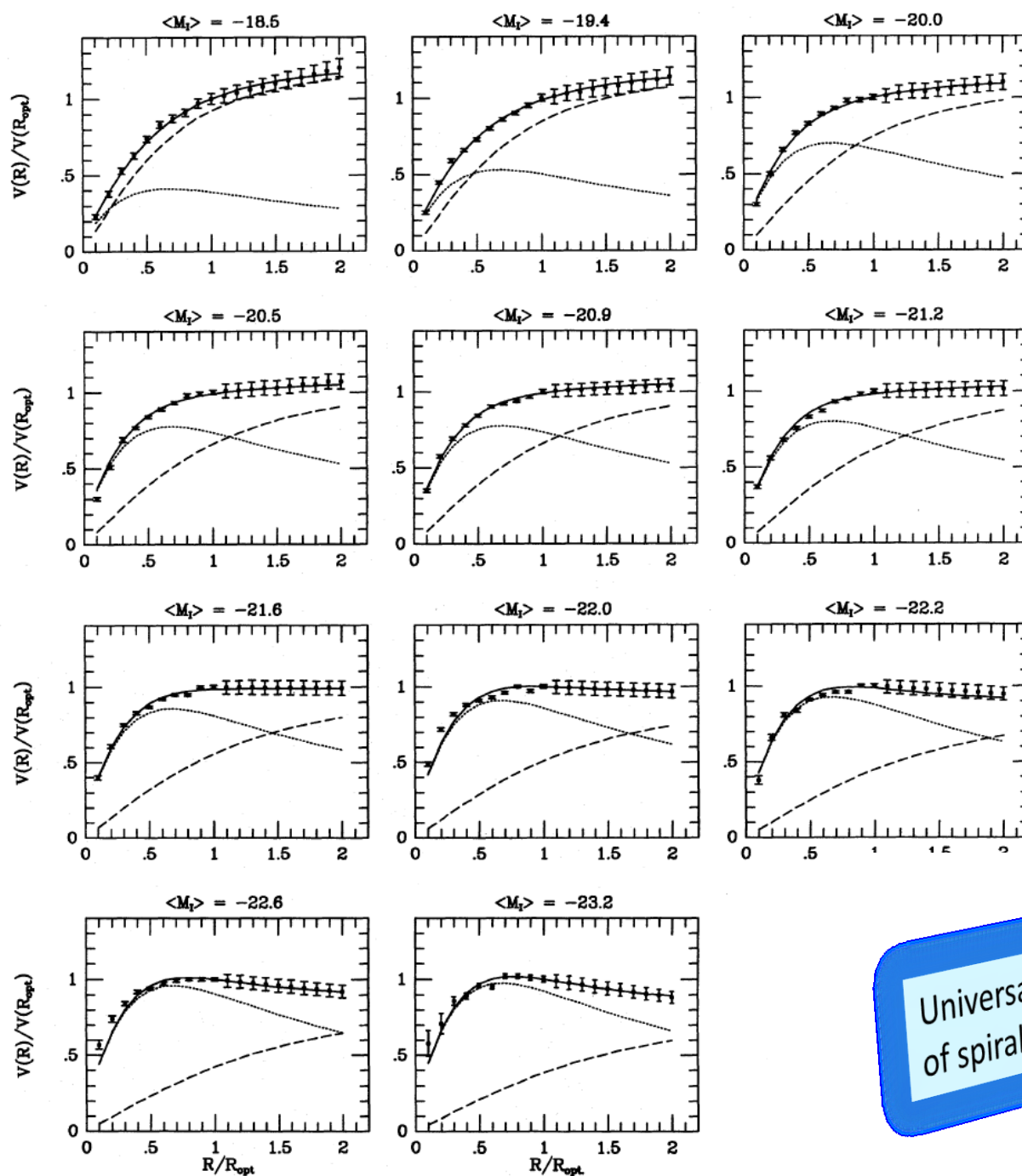


Figure A1. The luminous mass profiles for the galaxies in Sample B, grouped by luminosity bins. For each individual object, the light profile $L(r) \propto \int_0^r I(r') r' dr'$ is normalized to its total value L_{tot} ; the radius is normalized to R_{opt} . Grouping the light profiles by velocity amplitude yields a similar result.



Rotation curves are **not** self-similar with luminosity!

Figure 1. Synthetic rotation curves for Sample B arranged by luminosity. Galactocentric radii are normalized to R_{opt} , the radius encompassing 83 per cent of the total I luminosity. The last panel shows the rotation curve predicted for a pure self-gravitating exponential thin disc.



Smooth progression
of RC shape, and
disk/halo interplay,
with luminosity

Universal Rotation Curve
of spiral galaxies

Figure 6. Best two-component fits to the universal rotation curve (dotted line: disc; dashed line: halo)

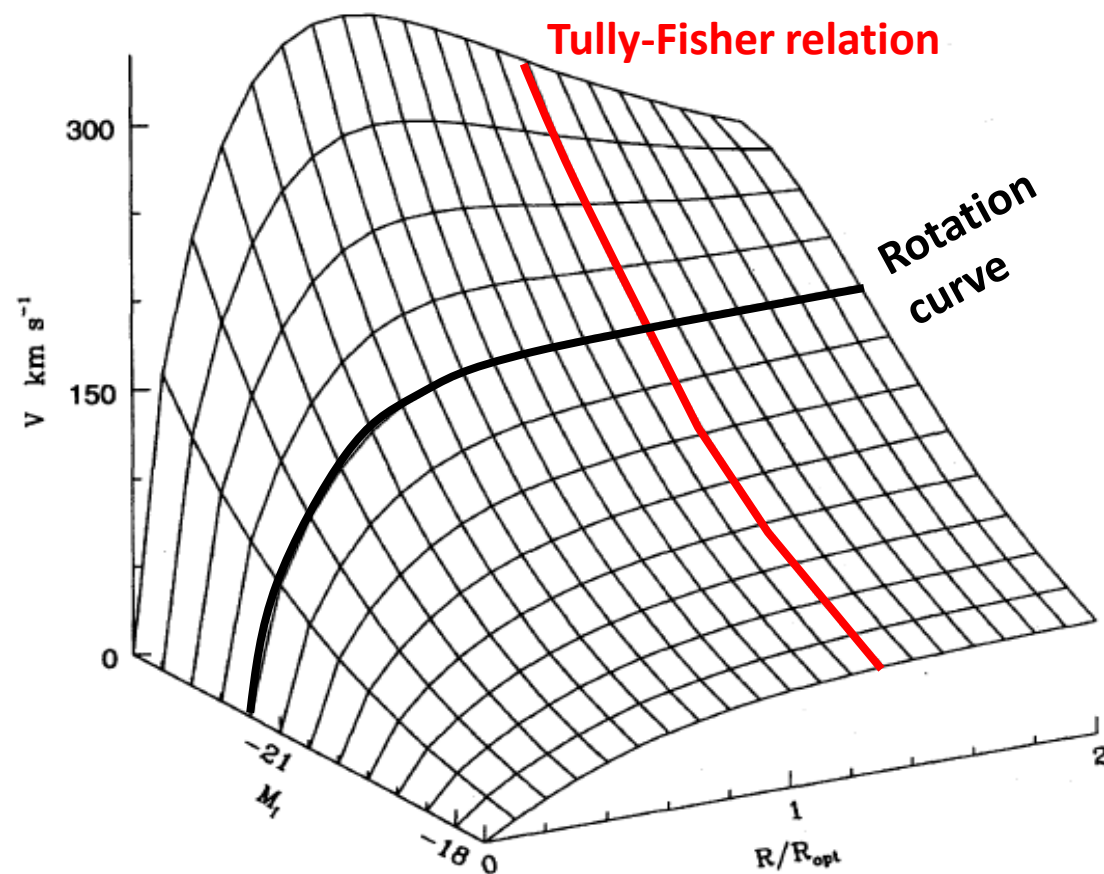
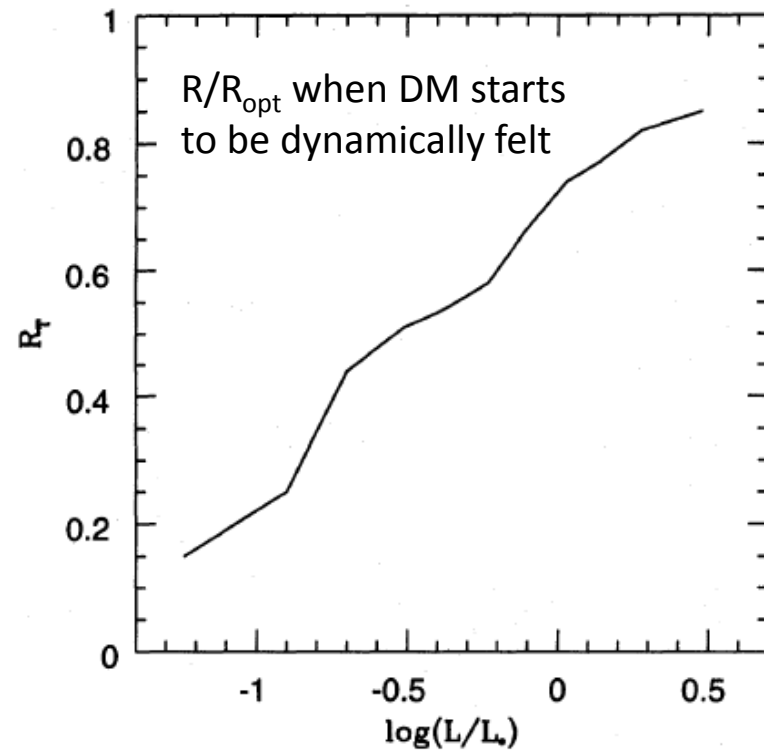


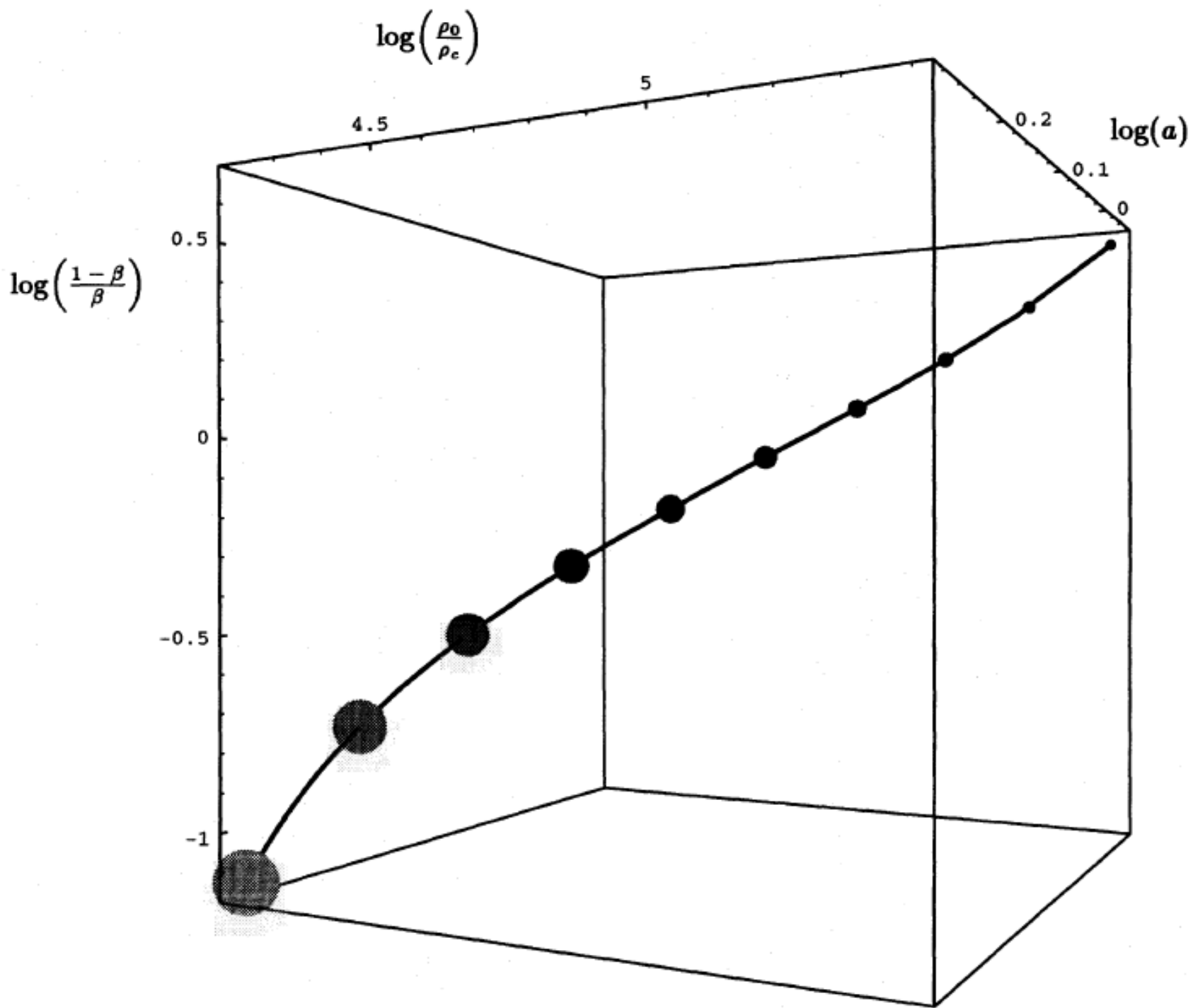
Figure 10. The URC surface.



$$\frac{\text{dark mass}}{\text{visible mass}} = 0.4 \left(\frac{L}{L_*} \right)^{-0.9}$$

$$\text{halo mass} = 1.6 \times 10^{12} \left(\frac{L}{L_*} \right)^{0.56} M_{\odot}$$

$$\frac{\text{halo central density}}{\text{critical density}} = 3.5 \times 10^4 \left(\frac{L}{L_*} \right)^{-0.7}$$



Whence these properties?

- Bottom-up cosmology: small galaxies formed first, hence their density retains the cosmological density at the epoch of their turnaround ($\delta\rho/\rho \sim 1.8$).

- Baryon infall: SF \rightarrow SN expl. \rightarrow winds \rightarrow most of infalling baryons **lost** in small gals., but **retained** in bigger ones.

- Smaller, denser gals. have little/no SF – bigger, less dense gals. do have gas and SF.

Small, nearby galaxies ... or ... large, faraway clusters?

Let's start from signal from self-interacting DM decay

$$\Phi_{\epsilon}^{PP}(> E_0) = \frac{1}{4\pi} \frac{\langle \sigma_{\text{ann}} v \rangle}{2m_{\chi}^2} \int_{E_0}^{m_{\chi}} \sum_{i=1}^n B^i \frac{dN_{\gamma}^i}{dE} dE$$

$$\Phi(> E_0, \Delta\Omega) = \Phi_{\epsilon}^{PP}(> E_0) J(\Delta\Omega) D^{-2}$$

→ small distances best!

$$J(\Delta\Omega) = \int_{\Delta\Omega} \int_{los} \rho^2(r(s, \Omega)) ds d\Omega$$

→ small guys win!

→ cosmology: dSph **halos** are best candidates for DM signal

→ astrophysics: dSph **stellar pops.** are most silent astroph bkgd

→ Dwarf Spheroidals: ideal DM candidates

Milky Way satellites → nearby
High M/L → DM dominated
Old stellar pop. → no ongoing SF

DSph	D_{\odot} (kpc)	L ($10^3 L_{\odot}$)	M/L ratio	Reference	Best positioned IACTs
Carina	101	430	40	[10]	HESS, CANGAROO
Draco	82	260	320	[10]	MAGIC , VERITAS
Fornax	138	15500	10	[10]	HESS, CANGAROO
Sculptor	79	2200	7	[10]	HESS, CANGAROO
Sextans	86	500	90	[10]	HESS, CANGAROO
UMi	66	290	580	[10]	MAGIC , VERITAS
Sagittarius*	24	58000	25	[10, 11]	HESS, CANGAROO
Coma Berenices	44	2.6	450	[12]	MAGIC , VERITAS
UMa II	32	2.8	1100?	[12]	MAGIC , VERITAS
Willman 1	38	0.9	700	[12]	MAGIC , VERITAS
Segue 1 [†]	23	0.3	>1320	[13]	MAGIC , VERITAS

* Not a dSph, but listed here because of its traditional interest for DM searches.

Example: Draco dSph modeling

$d \sim 80$ kpc

Bergström & Hooper 2006

total DM
annihil. rate

$$\Phi_A = \int_{r_{min}}^{r_a} dr 4\pi r^2 \frac{\langle \sigma_{Av} \rangle}{2} \left(\frac{\rho(r)}{m_\chi} \right)^2$$

$\langle \sigma_{Av} \rangle$, m_χ WIMP annihil. cross section, mass

γ -ray flux

$$F_\gamma = \frac{\Phi_A N_\gamma}{4\pi D^2} \quad N_\gamma \text{ rays / annihil}$$

$$y = r/r_s$$

upper limit

cusped
profile

$$\rho(r) = \frac{\rho_0}{y(1+y)^2}$$

$$F_\gamma = \frac{\rho_0^2 r_s^3 N_\gamma \langle \sigma_{Av} \rangle}{3m_\chi^2 D^2} \left[\frac{1}{(1+y_{min})^3} - \frac{1}{(1+y_a)^3} \right]$$

cored
profile

$$\rho(r) = \frac{\rho_0}{(1+y)(1+y^2)}$$

$$F_\gamma = \frac{\rho_0^2 r_s^3 N_\gamma \langle \sigma_{Av} \rangle}{4m_\chi^2 D^2} \left[\frac{2+y_{min}+y_{min}^2}{1+y_{min}+y_{min}^2+y_{min}^3} + \arctan(y_{min}) - \frac{2+y_a+y_a^2}{1+y_a+y_a^2+y_a^3} - \arctan(y_a) \right]$$

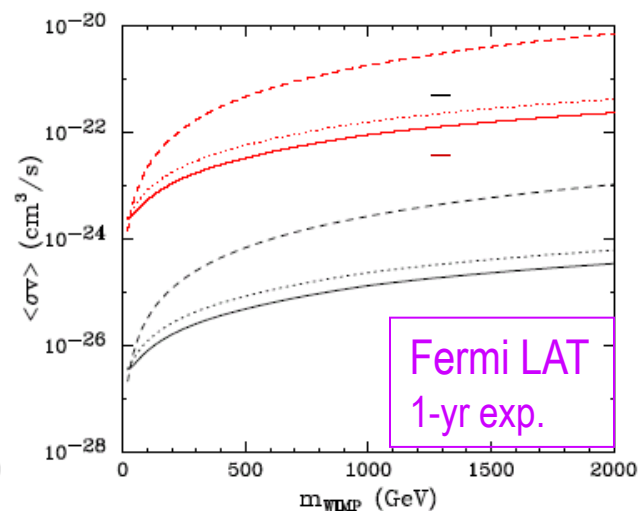
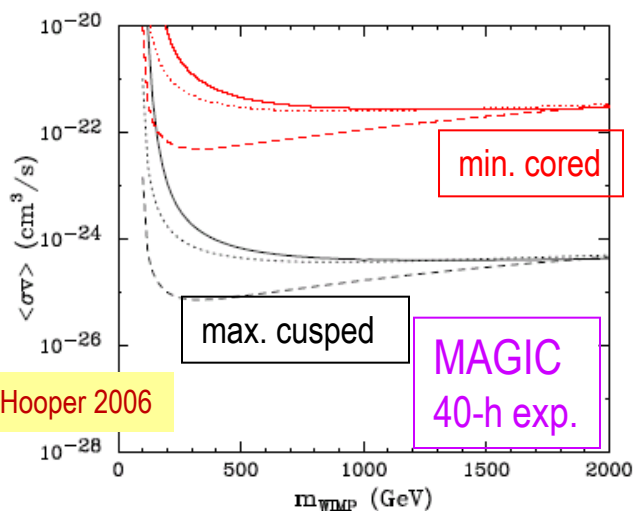
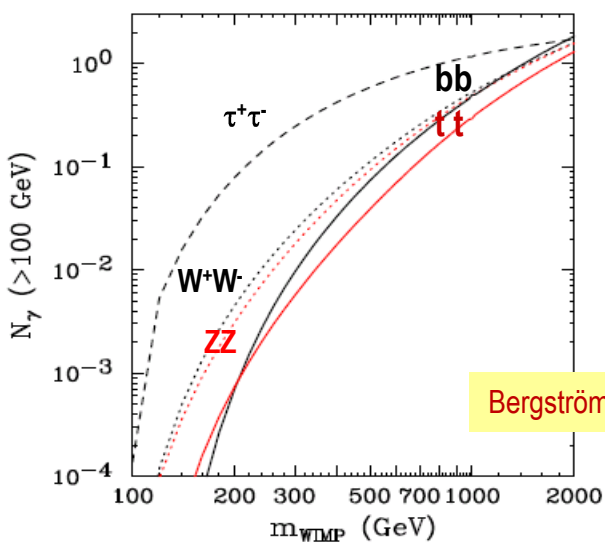
γ -ray flux

$$F_\gamma = \frac{\rho_0^2 r_s^3 N_\gamma \langle \sigma_{Av} \rangle}{3m_\chi^2 D^2} \times A$$

↑ part. phys
↑ astrophys

Profile Type	$A(r_a = r_s)$	$A(r_a \gg r_s)$
NFW	0.875	1.0
Core	0.160	0.323
Cusp, $\gamma = 1.1$	1.29	1.52
Cusp, $\gamma = 1.2$	2.16	2.63
Cusp, $\gamma = 1.3$	4.03	4.12
Cusp, $\gamma = 1.4$	11.1	12.5
Cusp, $\gamma = 1.45$	25.7	27.4

$r_s = 7 - 0.2$ kpc
 $\rho_0 = 10^7 - 10^9 M_\odot \text{ kpc}^{-3}$
 $\rho_0^2 r_s^3 = 0.03 - 6 M_\odot^2 \text{ kpc}^{-3}$



$$F_{\gamma, \text{NFW}}^{\text{max}} \approx 2.4 \times 10^{-10} \left(\frac{100 \text{ GeV}}{m_\chi} \right)^2 \left(\frac{\langle \sigma_A v \rangle}{3 \cdot 10^{-26} \text{ cm}^3 \text{ s}^{-1}} \right) \left(\frac{N_\gamma}{10} \right) \text{ cm}^{-2} \text{ s}^{-1}$$

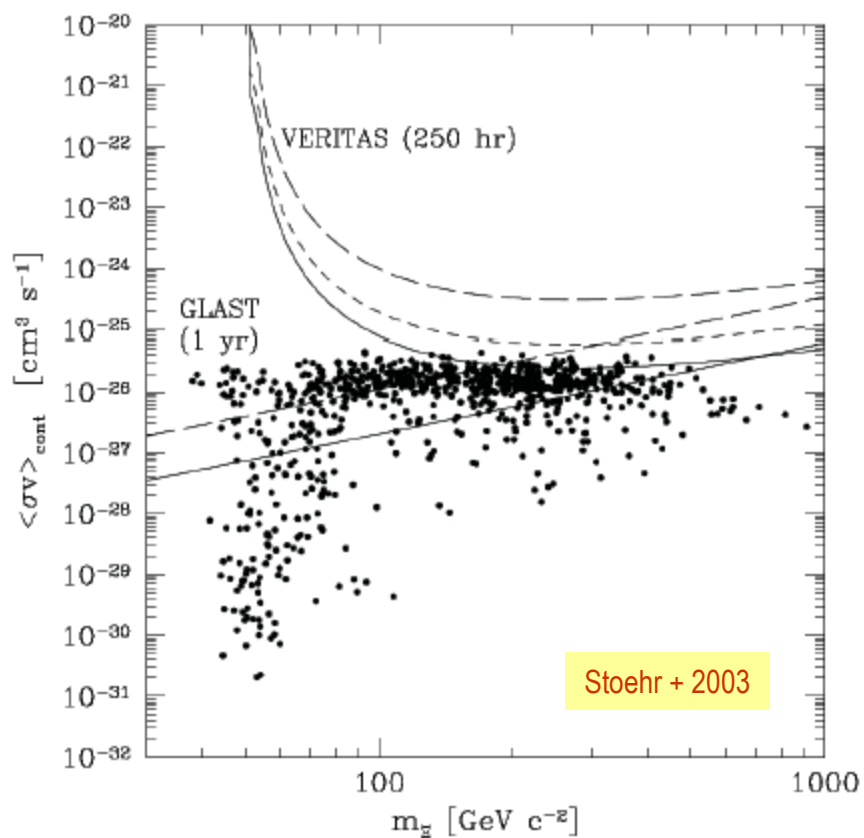
$$F_{\gamma, \text{NFW}}^{\text{min}} \approx 9.8 \times 10^{-13} \left(\frac{100 \text{ GeV}}{m_\chi} \right)^2 \left(\frac{\langle \sigma_A v \rangle}{3 \cdot 10^{-26} \text{ cm}^3 \text{ s}^{-1}} \right) \left(\frac{N_\gamma}{10} \right) \text{ cm}^{-2} \text{ s}^{-1}$$

$$F_{\gamma, \text{core}}^{\text{max}} \approx 4.2 \times 10^{-11} \left(\frac{100 \text{ GeV}}{m_\chi} \right)^2 \left(\frac{\langle \sigma_A v \rangle}{3 \cdot 10^{-26} \text{ cm}^3 \text{ s}^{-1}} \right) \left(\frac{N_\gamma}{10} \right) \text{ cm}^{-2} \text{ s}^{-1}$$

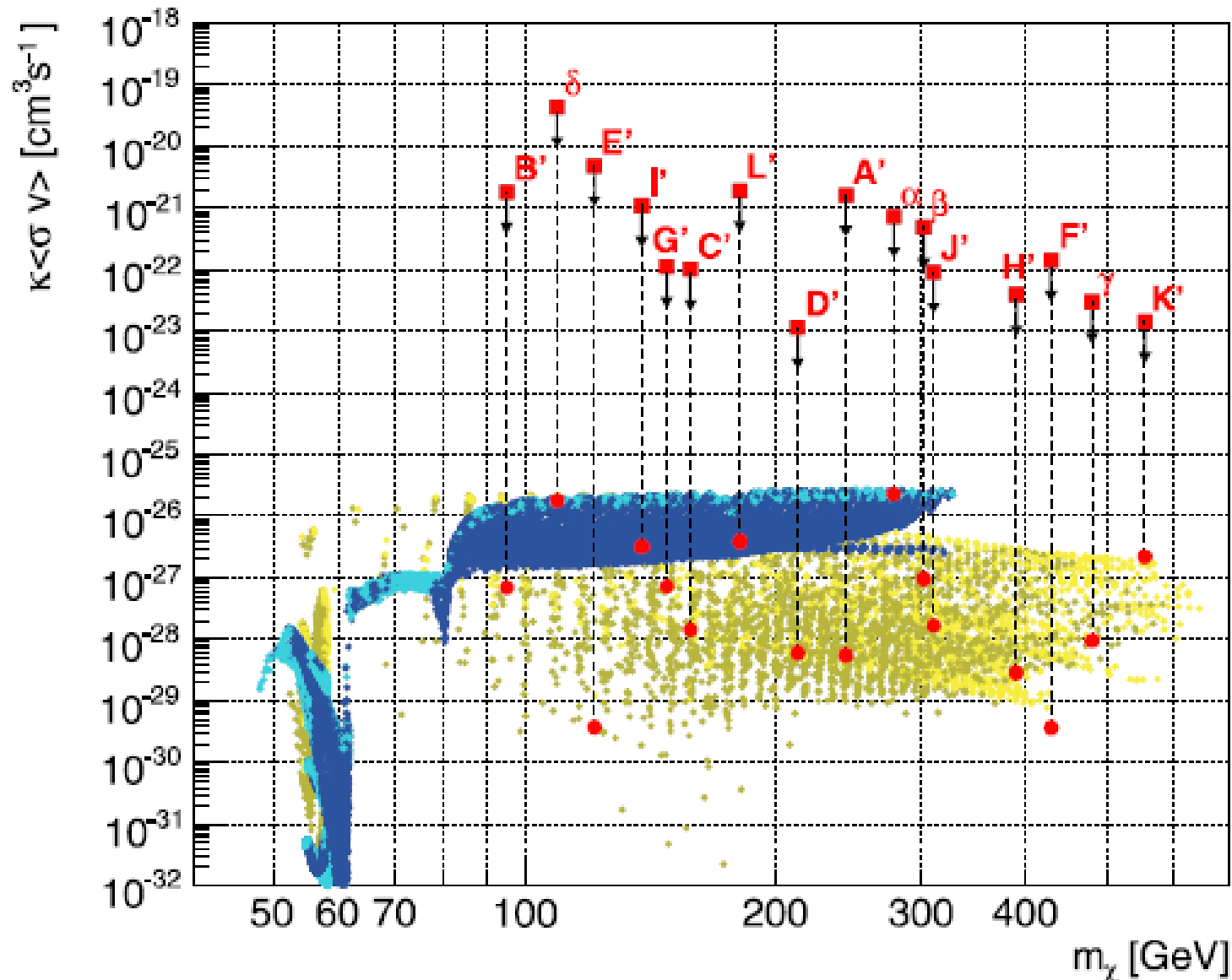
$$F_{\gamma, \text{core}}^{\text{min}} \approx 3.5 \times 10^{-13} \left(\frac{100 \text{ GeV}}{m_\chi} \right)^2 \left(\frac{\langle \sigma_A v \rangle}{3 \cdot 10^{-26} \text{ cm}^3 \text{ s}^{-1}} \right) \left(\frac{N_\gamma}{10} \right) \text{ cm}^{-2} \text{ s}^{-1}$$

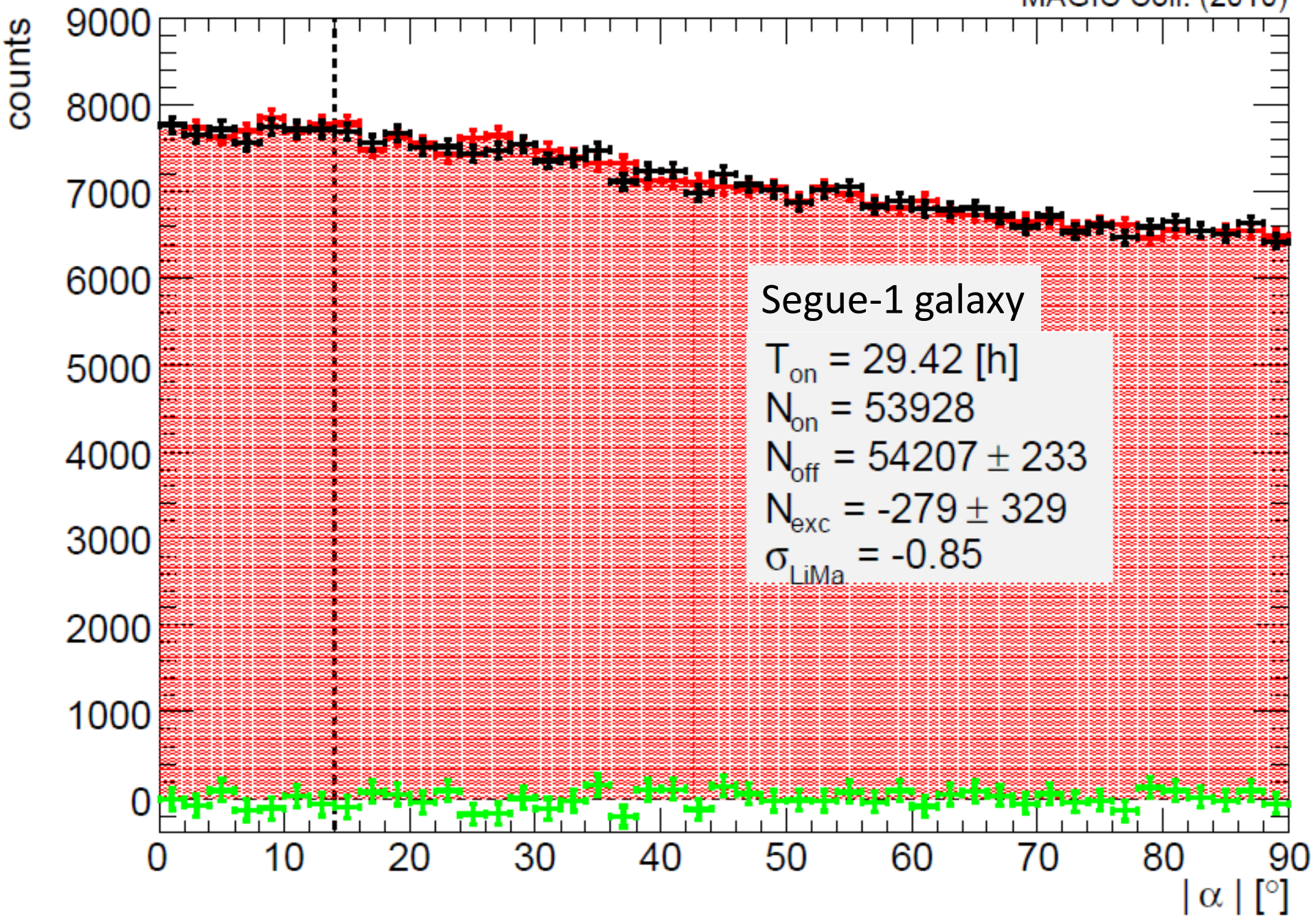
IACT neutralino detection:

$$\langle \sigma_A v \rangle \geq 10^{-25} \text{ cm}^3 \text{ s}^{-1}$$



Draco dSph obs'd *MAGIC* Albert et al. 2008





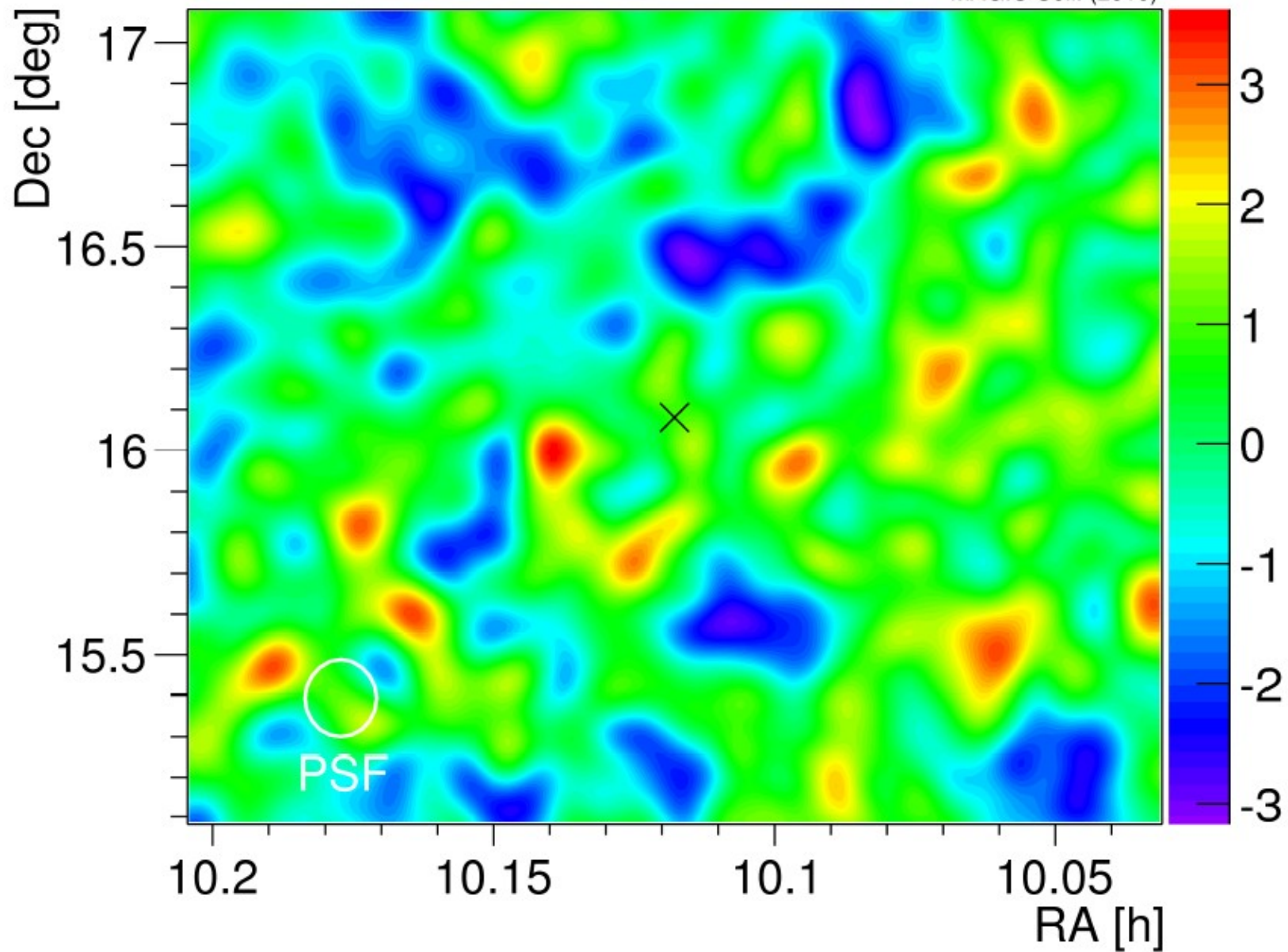
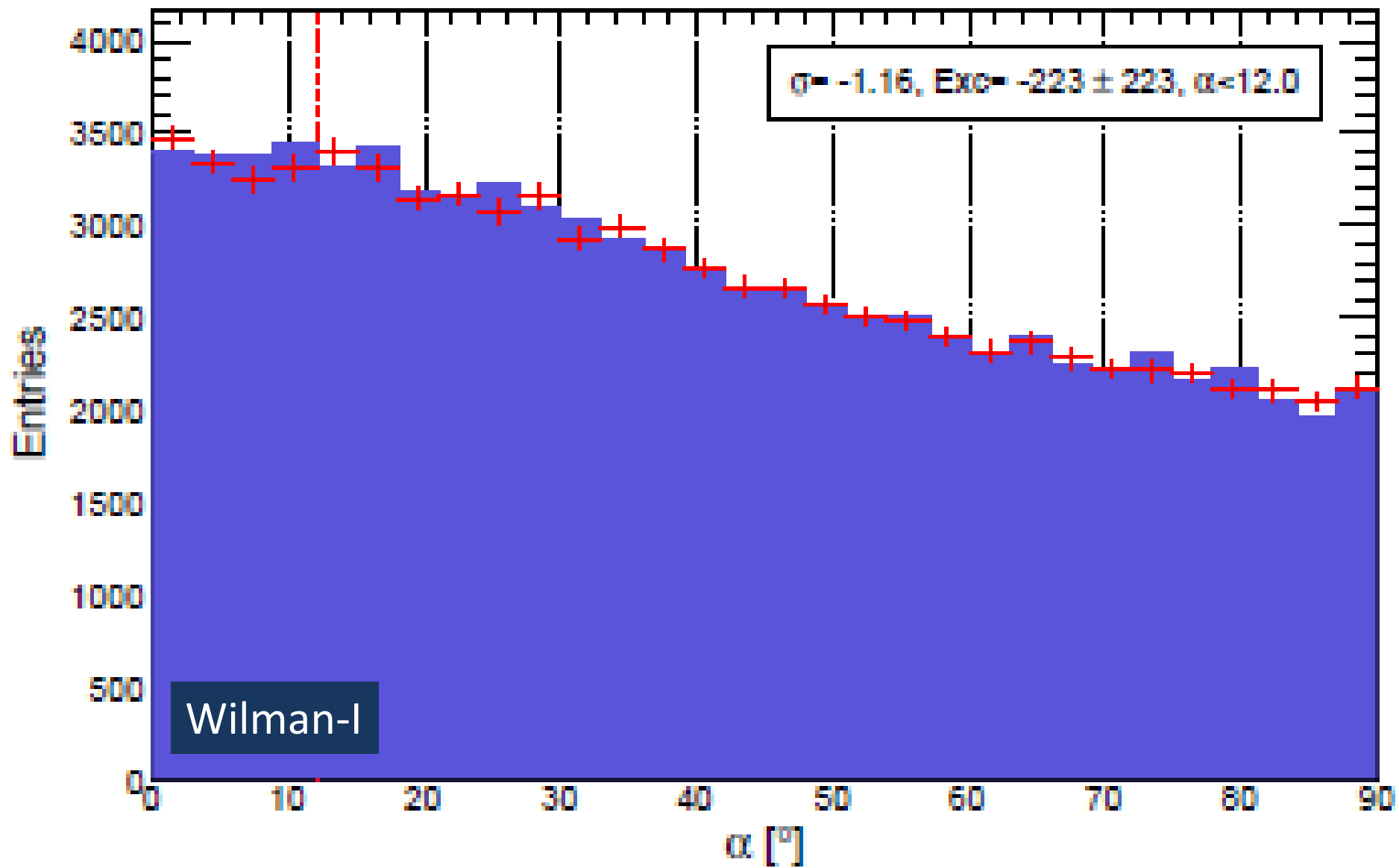


Figure 2. Significance map for events above 200 GeV in the Segue 1 sky region. The black cross marks the position of Segue 1 and the telescope PSF is also shown. The significance distribution is consistent with background fluctuations.



Summary

Galaxies can produce VHE γ rays, related to ongoing SF and DM decay

SF: γ emission detected from nearby starburst (M82, NGC253), quiescent (M31, LMC, SMC), and SB/Seyfert-I (NGC1068, NGC4945) galaxies.

CR energy densities: measured directly from γ emission and indirectly from radio emission, estimated from SR frequencies
→ results agree.

DM: no signal from MW center and from (best candidate) MW satellite dSph galaxies.
→ hunt ongoing ...